THE HUMAN MELANOMA-ASSOCIATED ANTIGEN p97 IS ATTACHED TO THE PLASMA MEMBRANE BY A GLYCOSYL-PHOSPHATIDYLINOSITOL ANCHOR

by

MICHAEL ROBERT FOOD

B.Sc., The University of Victoria, 1986

A THESIS SUBMITTED IN PARTIAL FULFILLMENT OF

THE REQUIREMENTS FOR THE DEGREE OF

MASTER OF SCIENCE

in

THE FACULTY OF GRADUATE STUDIES

(Biotechnology Laboratory and the Department of Microbiology)

We accept this thesis as conforming

to the required standard

THE UNIVERSITY OF BRITISH COLUMBIA

October 1992

In presenting this thesis in partial fulfilment of the requirements for an advanced degree at the University of British Columbia, I agree that the Library shall make it freely available for reference and study. I further agree that permission for extensive copying of this thesis for scholarly purposes may be granted by the head of my department or by his or her representatives. It is understood that copying or publication of this thesis for financial gain shall not be allowed without my written permission.

Department of _MICROBIOLOGY_

The University of British Columbia
Vancouver, Canada

Date _OCTOBER 15, 1992._

ABSTRACT:

Melanotransferrin, or p97 is a cell surface glycoprotein which was first described as a marker antigen for human melanoma cells. Although p97 has a high level of amino acid sequence homology to human serum transferrin and lactoferrin its function has not yet been determined. One feature that distinguishes p97 from the other members of the transferrin family is the presence of a stretch of 24 hydrophobic amino acids at the C-terminus. In all previous studies, this sequence was thought to form a proteinacious transmembrane domain. In this study, however, sensitivity to bacterial phosphatidylinositol-specific phospholipase C, biosynthetic labelling with [^{3}H]-ethanolamine, and partitioning in Triton X-114, were used to establish that p97 is expressed at the cell surface as a glycosyl-phosphatidylinositol anchored protein. As well, this anchor was shown to be present in p97 on human tumor lines and it apparently confers no special intracellular transport properties on the molecule. These findings raise important questions about the function of p97 and the possible involvement of this protein in a cellular iron uptake system that is independent from the transferrin/transferrin receptor system.

TABLE OF CONTENTS:

LIST OF TABLES:

LIST OF FIGURES:

ACKNOWLEDGEMENT:

LIST OF ABBREVIATIONS:

The abbreviations used are: UVR, ultraviolet radiation; Tf, transferrin; TR, transferrin receptor; MAb, monoclonal antibody; MAbs, monoclonal antibodies; GPI, glycosyl-phosphatidylinositol; VSG, variable surface glycoprotein; PI-PLC, phosphatidylinositol-specific phospholipase C; BFA, Brefeldin A; ATCC, American Type Culture Collection; DMEM, Dulbecco's Modified Eagle Medium; FBS, Fetal Bovine Serum; CHO, Chinese Hamster Ovary; FACS, fluorescence activated cell sorting; SDS-PAGE, sodium dodecyl sulfate-polyacrylamide gel electrophoresis; biotin, biotinamidocaproate N-hydroxysuccinimide ester; PMSF, phenylmethylsulfonylfluoride, MEM, Minimum Essential Medium.

INTRODUCTION:

The increase in the occurence of skin diseases in many industrialized nations has been attributed in large part to the increased exposure of the population to ultraviolet radiation (UVR) present in sunlight (1). The damage which results from this exposure to UVR can include: erythema, sunburn, photodamage, photocarcinogenesis, eye damage, immune system alterations, and chemical hypersensitivity (2). The most common skin cancers produced by exposure to UVR are the non-melanoma skin cancers, which are termed basal cell and squamous cell carcinomas (2). These cancers have been associated with repeated sun exposure (3). The less common skin cancer, cutaneous malignant melanoma, has been associated with shorter, more intense exposure to the sun (4). This form of skin cancer is both rapidly increasing and highly fatal, in fact, it has been suggested that by the year 2000, approaching 1 in a 100 caucasians will develop malignant melanoma, and 20-30% of these people will ultimately die from it (5). The variety of risk factors which contribute to the development of malignant melanoma have not been completely described.

Iron is required by all cells (6), consequently many different systems have been developed to obtain iron from the environment. Two problems which any system must address are that free iron is toxic and that iron chemistry favors the production of insoluble and inaccessible hydroxides (7). Iron is a component of a large number of proteins with essential cellular functions, thus, it is absolutely required for cell proliferation (6). Iron transport into microorganisms can be mediated by a high affinity system consisting of a soluble iron ligand (siderophore), a membrane bound receptor (ferri-siderophore), and an enzymatic release mechanism, as well as by an iron reductase system (8).

In vertebrates, the iron requirement is thought to be provided by the binding of iron to the major serum iron transport protein called transferrin (Tf). The Tf molecule is a monomeric glycoprotein of 80,000 daltons molecular mass (9). It can reversibly bind two Fe^{3+} ions per molecule, simultaneously with two CO_3^{2-} ions (9). Evidence from the Tf sequence and proteolytic digestion suggest that the molecule can be subdivided into two homologous domains of approximately 340 amino acids which share 35-40% sequence identity to one another (9). Each domain has a single iron binding site which suggests that the transferrins evolved by gene duplication of a single iron binding domain (9). The currently accepted view is that soluble Tf binds iron and this complex interacts with the transferrin receptor (TR) on the plasma membrane (10). The TR is composed of two identical disulfide linked polypeptide chains, each with a molecular mass of 95,000 daltons (10). The efficiency of this mechanism is increased because the TR can bind two molecules of iron-Tf per receptor (6). After binding, the iron-Tf/TR complex remains membrane associated and is concentrated in coated pits and internalized. The resulting endosomes become acidified and the iron, likely Fe^{3+}, is released from the complex (10). The apotransferrin remains bound to the receptor and is recycled to the cell surface where it is released at neutral pH and can participate in the binding and uptake of additional iron into the cell (6). The iron in the acidified endosome is transported across the endosomal membrane by an uncharacterized mechanism, where it serves as a substrate for the biosynthesis of iron containing proteins or is stored in ferritin deposits (10). Although cellular iron uptake has been shown to be mediated mainly by the Tf/TR pathway (11), there is evidence for non-Tf mediated pathways of iron incorporation in leukemic cells (12), HeLa cells

(13,14), and in hepatocytes (15). In human melanoma cells, a non-Tf mediated pathway has also been investigated (16-19).

Melanotransferrin, also known as the human melanoma-associated antigen p97, was one of the first cell surface markers associated with human skin cancer (20). The p97 molecule was characterized using monoclonal antibodies (MAb) raised against melanoma cells (20-22), including the SK-MEL-28 cell line, and p97 has been termed a melanoma specific marker. It was shown to be a monomeric membrane bound protein with a molecular mass of 97,000 daltons (23). The p97 molecule was proposed to be both a predictive marker for melanomas, and the target site for immunotherapy (24). Subsequent work with p97 on SK-MEL-28 cells revealed that it was capable of binding iron (25). Furthermore, p97, like Tf and the TR, is a sialoglycoprotein, which is encoded on chromosome 3 in humans (26). The primary structure of p97 deduced from its mRNA sequence (27) indicated that it belongs to a group of closely related iron binding proteins found in vertebrates. This family includes serum Tf, lactoferrin, and avian egg white ovotransferrin. The human p97 and lactoferrin molecules are known to share 40% sequence identity (9). In contrast to the other molecules of the Tf family, p97 is the only one which is directly associated with the cell membrane, which has implications for the evolution of the Tf family and, potentially, for iron transport mechanisms in general.

The p97 molecule was described independently by other investigators. It was shown that p97 was the same as the gp95 molecule (23), described by Dippold (28). Subsequently, the gp87 molecule was also shown to be identical to the p97 molecule (29). More recently, a unique tumor antigen of human melanoma was described in detail, and designated gp90 (30). This antigen was shown to be expressed in high quantities on the surface of a wide variety of

cultured cells, but only in small quantities on cells of a limited range of normal tissues (30). It was not until 1989 that it was demonstrated that this unique antigen was in fact p97 and not a new melanoma-associated antigen (31). One benefit of these studies is that a large number of unique MAb to p97 were generated, which collectively defined many different epitopes of the molecule.

The distribution of the p97 molecule has been described in considerable detail over the last twelve years. The first quantitative analysis of p97 expression in normal and neoplastic tissues showed that it was present in large amounts in most melanomas, some tumors and certain fetal tissues, but in normal tissues it was expressed in small amounts (21). Further work by the same group again demonstrated that p97 was expressed by cells from melanoma tumor biopsies but not in normal adult tissues (22). One interesting observation was that p97 was present in high quantities in the fetal colon, lung and umbilical cord (22). In subsequent years the distribution of the p97 molecule continued to be investigated, most notably in the form of a comparative study of antigen expression in a variety of cell types (32). The p97 molecule was again shown to be present on the cell surface of a number of melanoma and other cancer lines, and absent on the cell surfaces of a wide variety of normal adult tissues (32). An exhaustive study of the expression of the p97 molecule in cultured tumor and normal cells (30) showed that p97 was expressed at a high level in cell lines ranging from melanoma to colon, kidney and lung cancer; moreover, in normal cells, only melanocytes, kidney epithelium and fibroblasts showed a degree of p97 expression. It has been suggested that the distribution of expression of the p97 molecule indicates that p97 is actually an oncogene.

The situation is not as clear as the majority of these results would seem to indicate. It has subsequently been shown that the p97 molecule is expressed on endothelial cells of the human liver (33). The localization of the p97 molecule was also shown to be distinct from that of Tf and the TR (33). As well, p97 was found to be present on central vein walls in fetal liver tissue, which was not demonstrated previously (33). These findings are important because they are the first reports of the presence of the p97 molecule on the cell surface of tissues which were previously believed to express none of the molecule. In our own laboratory, it has been shown that the p97 molecule is expressed by capillary endothelial cells in the normal human brain (Food et al, unpublished observations). As with the liver data, this finding contradicts previously published data. It would appear, then, that the p97 molecule may be distributed in normal tissues as well as in all of the cancer tumors and cell lines which have been previously described.

While p97 does not appear to be as strictly tumor specific as was once believed, there have been several investigations on the possible immunotherapeutic properties of the molecule. It was shown that conjugates of an anti-p97 MAb and the toxin, ricin A-chain, were useful in killing human melanoma cells which expressed p97 at more than 80,000 molecules per cell (34). This effect was not evident in cells which expressed less than 5,000 molecules of p97 per cell, indicating that the presence of p97 at low levels in normal tissues may not be a factor when considering the efficacy of immunotoxins (34). The construction of a recombinant vaccinia virus, which was shown to cause infected tissue culture cells to express p97 at a high level, allowed the investigators to attempt to immunize against melanoma (35). It was found that the immunization of both mice and monkeys with the recombinant construct resulted in both humoral and cell mediated immune

responses (36). Monkeys are known to express a low level of cross-reactive p97 (36), therefore, it appears that the low level of p97 expression in normal tissues does not interfere with the therapeutic effect being investigated. Another model involving mouse melanoma metastases has also been investigated (24). In this case the generation of a T-cell population reactive to p97 was observed, after immunization with the recombinant vaccinia virus construct. The result of subsequent adoptive therapy experiments was that pulmonary melanoma metastases were eradicated in mice treated with these T-cells (24). There appears, then, to be some potential for the use of p97 as a target for various therapeutic reagents despite differing interpretations of the normal distribution status of the molecule.

In addition to the Tf-like domain, the deduced sequence of p97 has a hydrophobic segment at its C-terminal which was thought to allow the molecule to be inserted into the plasma membrane (27). Using the Eisenberg algorithm (37), which predicts membrane associated domains, analysis of the putative proteinacious membrane attachment segment of the p97 molecule has been completed (Food et al, unpublished observations). This analysis suggests that the putative transmembrane domain of the p97 protein will not act as a membrane anchor, which implies that p97 is anchored to the plasma membrane by a different mechanism. Though the results of this analysis have never been interpreted in this manner, further investigation revealed that if a hydrophobic-like transmembrane region is present in a monomeric protein but not predicted to be a hydrophobic transmembrane domain by this algorithm, the examined protein is likely attached by a glycosyl-phosphatidylinositol (GPI) anchor. This analysis has been consistent for a number of GPI-anchored proteins, including Thy-1, Ly-6 and Qa-2 (Food et al, unpublished observations).

Classically, plasma membrane associated proteins are imbedded in the membrane via a hydrophobic interaction between the lipid bilayer and either an alpha helical transmembrane polypeptide segment or a less complex stretch of hydrophobic or uncharged residues (38). Recently, however, many proteins have been described that are attached to the plasma membrane via a GPI-anchor (38). Proteins with GPI-anchors have been detected in a variety of organisms ranging from mammals to protozoa, insects, slime molds, and yeast, but not fungi, bacteria and higher plants (38). As well, GPI-anchored proteins have been described in a variety of cell types, exhibiting considerable diversity in both functional and evolutionary terms (39).

The general structural features of GPI-anchors have been summarized (Figure 1). Briefly, the C-terminal amino acid of the protein is linked through the α-carboxyl group via an amide linkage to the amino group of the phosphoethanolamine moiety of the GPI-anchor. The phosphoethanolamine moiety is then linked to a glycan, usually consisting of mannose and glucosamine, while the glucosamine is linked glycosidically to the inositol-containing phospholipid. The anchoring of the protein to the plasma membrane is carried out by phosphatidylinositol (38). The complete structure of several GPI-anchored proteins have been determined including the variable surface glycoprotein (VSG) from *Trypanosoma brucei* (40) and mammalian Thy-1(41). It is not surprising that the generalized structure for GPI-anchors is based on work done on these two molecules (38).

Many different procedures have been developed for the identification of GPI-anchored proteins. The most commonly used technique involves the use of the bacterial enzyme phosphatidylinositol-specific phospholipase C (PI-PLC) for the release of the GPI-anchored protein from the cell surface (38). Another technique involves biosynthetically labelling cells with radiolabelled

Figure 1: General structural features of the GPI-anchor.

The general structure of the GPI-anchor with the sites of enzyme action indicated. This figure has been adapted from the review of Ferguson and Williams (47). Abbreviations: AA: carboxy-terminal amino acid; EtN: ethanolamine; P: phosphate; glycan: variable carbohydrate portion; GlcNH2: glucosamine. Cleavage sites shown include: HNO2: nitrous acid deamination; GPI-PLD: site of GPI-PLD activity; PI-PLC/GPI-PLC: site of PI-PLC/GPI-PLC activity; PLA2: site of phospholipase A2 activity.
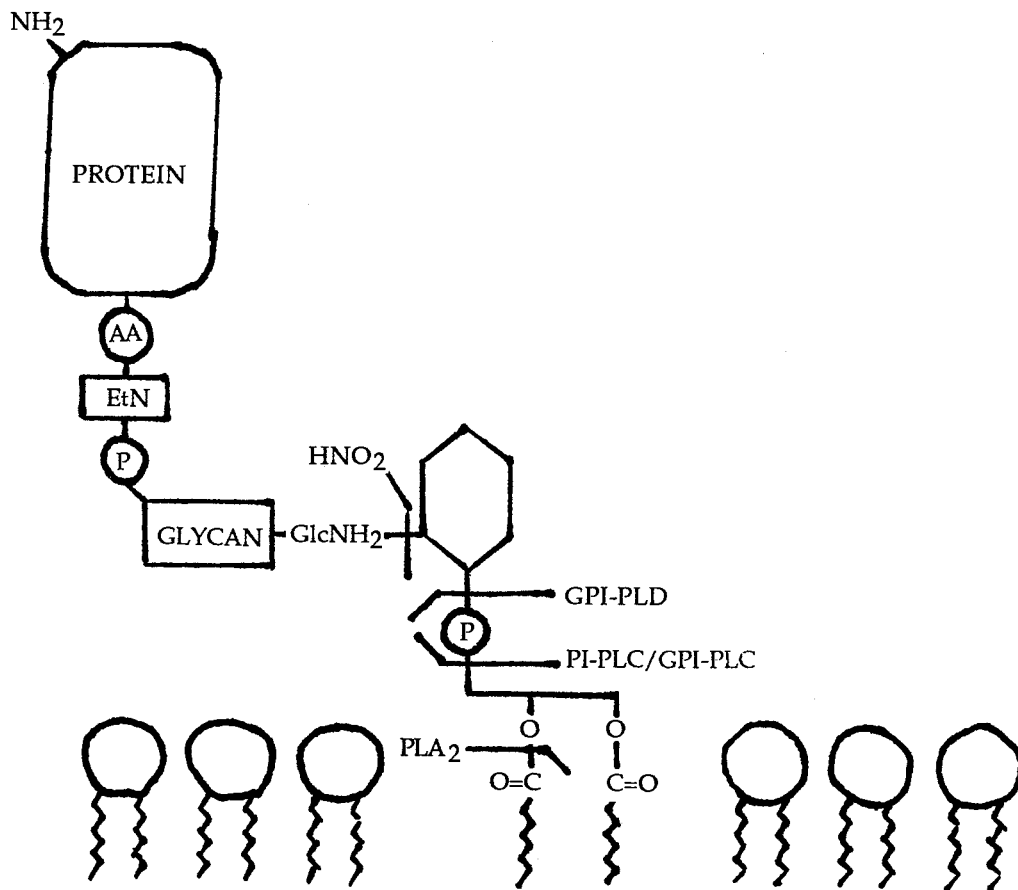
anchor components ([^{3}H]-ethanolamine, [^{3}H]-fatty acids, [^{3}H]-inositol, [^{32}P]-phosphate) (38). A further method involving cross reactive determinants on the released proteins has also been utilized. Generally, the presence of a GPI-anchor is proven by a variety of these methods rather than one in particular.

The biosynthesis of GPI-anchored proteins has also been described in some detail. It is known that the attachment of the protein to the GPI-anchor occurs within a minute of completion of polypeptide synthesis (42). Due to this rapid processing time, it is thought that the protein is attached to a preformed GPI-anchor, in the endoplasmic reticulum by a transamidase (38). The signal which directs the attachment of the GPI-anchor to the protein is thought to exist in the C-terminal region of the protein (38). There is no consensus sequence for the GPI-anchor attachment, the only features that occur regularly are that the C-terminal residues are moderately hydrophobic and that there are a pair of small residues placed 10-12 amino acids to the N-terminal side of this hydrophobic domain (43,44). It is thought that these are the only requirements for GPI-anchoring, and no other motifs are necessary (44). There have been experiments where the C-terminal regions of GPI-anchored proteins are switched with the same regions of standard hydrophobic transmembrane proteins, resulting, after processing, in the attachment of a GPI-anchor to these proteins (45). After the GPI-anchor has been attached to the protein there can also be post attachment events such as the addition of sugar side chains (38). There can also be defects in the GPI-anchor machinery which can, in some cases, result in the release of soluble forms of the protein. In fact, 8 different complementation groups with defects in the production of the Thy-1 molecule have been produced by immunoselection (46). Since the defect in only one of these classes is in the structural gene of Thy-1, the biochemical defects in each of the remaining

classes should constitute different elements of the GPI-anchor biosynthetic pathway.

One of the most interesting features of GPI-anchored proteins is that they can be released from the cell surface by the action of specific phopholipases. Several of these enzymes have been characterized, with the most common the bacterial PI-PLC. These enzymes cleave between the glycerol backbone and the phosphate group of the GPI-anchor (Figure 1) (47). There are also eukaryotic GPI-PLC which are membrane bound and cleave only GPI and not PI as is the case for the bacterial PI-PLC (38). These enzymes cleave the GPI-anchor at the same place as the bacterial PI-PLC (Figure 1). The final group is the eukaryotic GPI-PLD type of enzymes. Once again these enzymes are specific to the GPI-anchor only (38), cleaving between the inositol and the phosphate (Figure 1). While this enzyme has been found in the mammalian plasma, its activity on proteins from intact cell membranes is not known (48).

The fungal metabolite Brefeldin A (BFA) is known to have many different effects on the secretory pathway of mammalian cells (49). The effects of BFA are still a matter of some debate, but they can be briefly summarized in this manner: BFA affects the early secretory pathway, resulting in the inhibition of protein transport and the disassembly of the Golgi apparatus (50). It is the loss of the coat protein β-cop from Golgi membranes in the presence of BFA, followed by formation of tubular connections between the Golgi cisternae which results in movement of Golgi enzymes to the ER (49). It is also known that BFA affects the trans-Golgi network and the endosomal system (49). While BFA is known to inhibit the transport of membrane and secreted proteins to their appropriate destinations the effect on GPI-anchored proteins is not well documented.

In this work, the structure which is responsible for the attachment of the p97 molecule to the surface of melanoma cells was investigated.

MATERIALS AND METHODS:

Cell culture and Flow Cytometry:

The human melanoma line SK-MEL-28 (HTB 72) and the mouse lymphoma line EL-4 (TIB 39) were obtained from the American Type Culture Collection (ATCC). These lines were maintained in Dulbecco's Modified Eagle Medium (DMEM) supplemented with 10% fetal bovine serum (FBS), 20 mM HEPES, 100 U/ml penicillin, 100 μg/ml streptomycin, 2 mM L-glutamine, and 50 μM 2-mercaptoethanol. The Chinese Hamster Ovary (CHO) cell lines WTB and TRVB were obtained from Dr. F. Maxfield of New York University, New York City. These lines were maintained in Hams F12 medium supplemented with 10% FBS, 20 mM HEPES, 100 U/ml penicillin, 100 μg/ml streptomycin, and 2 mM L-glutamine. The transfected WTB and TRVB cell lines expressing human p97 were grown in the same media with the addition of G418 sulfate (Gibco) at a concentration of 800 μg/ml. All cell lines were incubated at 37°C in a 5% CO_2 humidified atmosphere. When necessary, adherent lines were released by treatment with versene.

L235 is a hybridoma cell line (HB 8446) from ATCC secreting a mouse MAb (IgG_1) that reacts with the human p97 molecule. OKT9 is a hybridoma cell line (CRL 8021) from ATCC that produces a mouse MAb (IgG_1) that reacts with the human TR. The T24/31.7 cell line was obtained from Dr. R. Hyman, of The Salk Institute, in San Diego. This hybridoma secretes a rat MAb (IgG_1) which reacts with mouse Thy-1. The γE1/9.9.3 cell line was obtained from Dr. F. Takei of The University of British Columbia, in Vancouver. This hybridoma secretes a rat MAb (IgG_1) which reacts with the mouse TR. In most cases tissue culture supernatants were used as the source of antibody.

The reactivity of the various MAbs to the human and mouse antigens of interest in this study were investigated. In these experiments the cells were

counted (10^6 cells/tube) and washed twice in fluorescence activated cell sorting (FACS) buffer, which consisted of DMEM containing 0.5% (wt/vol) bovine serum albumin, 20 mM HEPES, and 20 mM NaN_3. The cells were incubated with the various MAbs for 45 min at 4°C, then washed and labelled with the appropriate fluoresceinated secondary antibody for 45 min at 4°C. The cells were then washed and fixed in 1.5% (vol/vol) p-formaldehyde in PBS. A Becton-Dickinson FACScan flow cytometer was used to measure 5000 events per sample. The conversion of log scale to linear scale values was accomplished by using the formula: linear mean fluorescence = $10^{(log\ mean\ fluorescence/256\ channels)}$ (51). The fluorescence intensities were normalized with respect to unstained control samples and presented as mean linear fluorescences.

For some of the procedures in this work it was necessary to have a source of purified MAb. The tissue culture supernatants for MAb L235, C and OKT9 were centrifuged and filtered. The MAbs were then purified with a Protein G Sepharose column (MAbTrap G/Pharmacia) by the procedure recommended by the manufacturer. The purified MAb were then tested: for purity by sodium dodecyl sulfate-polyacrylamide gel electrophoresis (SDS-PAGE) under denaturing conditions, for protein concentration by spectrophotometry, and for activity by FACS.

Sensitivity of p97 to release by bacterial enzymes as shown by Flow Cytometry:

The purified PI-PLC used in this work was the kind gift of Dr. M. G. Low, of Columbia University in New York City. This enzyme was isolated from culture supernatants of *Bacillus subtilis* (BG2320), transfected with the PI-PLC gene from *Bacillus thuringiensis,* purified according to Low (52). A titration of purified bacterial PI-PLC activity on p97 on SK-MEL-28 cells ranged from 64% release (0.17 U/10^6 cells), to 88% release (0.85 U/10^6 cells), and 95%

release (1.7 U/10^6 cells). The purified PI-PLC was used at a concentration of 1.7 U/10^6 cells (17 U/ml) in FACS buffer. The crude PI-PLC was the unpurified culture supernatant from the *Bacillus subtilis* (BG2320) transfected with the PI-PLC gene from *Bacillus thuringiensis*. In the experiment 100 µl of the culture supernatant was used for 10^6 cells. The pronase used in this study was the Type XIV Protease from *Streptomyces griseus* (Sigma) at a concentration of 1 mg/ml in FACS buffer. In experiments involving these enzymes the cells were counted, washed twice in FACS buffer and then incubated with the enzyme preparation for 1h at 37°C. The cells were then labelled for, and analyzed by, FACS, as described in the flow cytometry section.

Phase partitioning in Triton X-114:

To investigate p97 partitioning in Triton X-114, the cell surface proteins of 8.0 x 10^6 cells were labelled with 0.4 mg biotinamidocaproate N-hydroxysuccinimide ester (biotin, Sigma) as described (53). The cells were washed several times in DMEM, divided into two samples that were incubated for 60 min at 6°C, in the presence or absence of PI-PLC (1.7 U/10^6 cells) respectively. Both the cell supernatant and the cell pellet were subsequently processed. The cells were washed once more and lysed in a buffer containing 10 mM Tris-HCl pH 7.4, 150 mM NaCl, 1% Triton X-114, 1 mM phenylmethylsulfonylfluoride (PMSF) and 100 µg/ml lysine to block biotin. Triton X-114 (Sigma) was precondensated as described (54). The same buffer was added to the supernatant. The samples were centrifuged at 12,000 g for 10 min at 4°C to remove the cell nuclei and cell debris. The phase separation was obtained by incubation at 30°C followed by a centrifugation at 3000 g for 3 min at room temperature. The samples were re-extracted 3 times in order to improve the separation and the corresponding phases were

pooled. The samples were precleared for 2 h with washed protein A-agarose and subsequently divided into two halves for immunoprecipitation of p97 and TR using L235 and OKT9 MAb respectively, followed by protein A-agarose precoated with rabbit anti-mouse IgG (Jackson ImmunoResearch). After immunoprecipitation, the samples were washed 6 times in 50 mM Tris-HCl pH 6.5, 150 mM NaCl, 2 mM EDTA, and 0.5% NP-40. The proteins were eluted from beads in SDS-PAGE loading buffer and separated on an 8% SDS-PAGE gel under reducing conditions. The proteins were transferred onto Immobilon membranes (Millipore) by electroblotting, and detected using peroxidase-conjugated streptavidin (Jackson ImmunoResearch) and the chemiluminescence ECL Western blotting detection system (Amersham) using the conditions recommended by the manufacturers.

Construction of transfectant cell lines expressing human p97:

The bacterial neomycin resistance gene, which confers resistance to G418 (Gibco) in mammalian cells, was contained in the pWJ218 construct (Figure 2A) from Dr. W. A. Jefferies and Dr. S. Kvist (unpublished). The human p97 expression vector pSV2p97a (Figure 2B), containing the entire coding region of p97 cDNA driven by the SV40 early promoter, was obtained from Dr. G. Plowman and Dr. K. E. Hellström, of Bristol-Meyers Squibb in Seattle (55). These plasmids were cotransfected into the WTB and TRVB lines by the Lipofectin method (Gibco) following the procedure recommended by the manufacturer. Using the appropriate antibodies, cell populations expressing p97 were analyzed by flow cytometry. These populations were further sorted for cells that expressed higher levels of p97 and then were sub-cloned by limiting dilution. The resultant cell lines were analyzed by FACS to ensure high expression levels of p97. The sensitivity of the p97 expressed by these lines to release by PI-PLC was then determined by FACS.

Figure 2: Summary of cDNA constructs used to transfect CHO lines.

A: pWJ218: This plasmid contains the neo-phosphotransferase gene located in the Tn 5 element, which confers resistance to the antibiotic G418 (geneticin), driven by the SV-40 early promoter.

B: pSV2p97a: This plasmid contains the entire coding region of the p97 gene, driven by the SV-40 early promoter/enhancer.

A
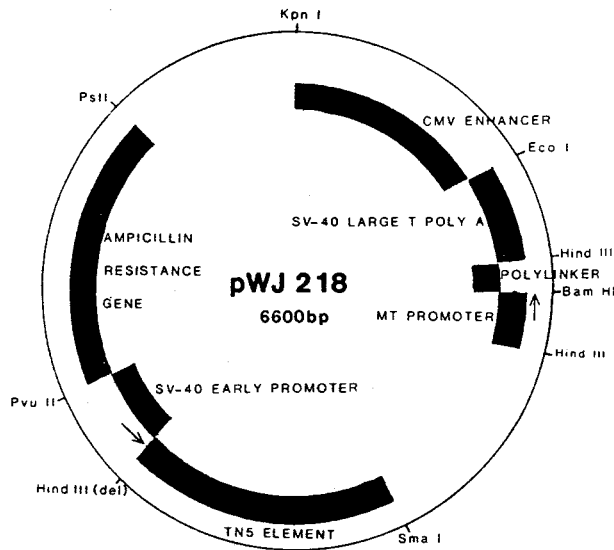
B
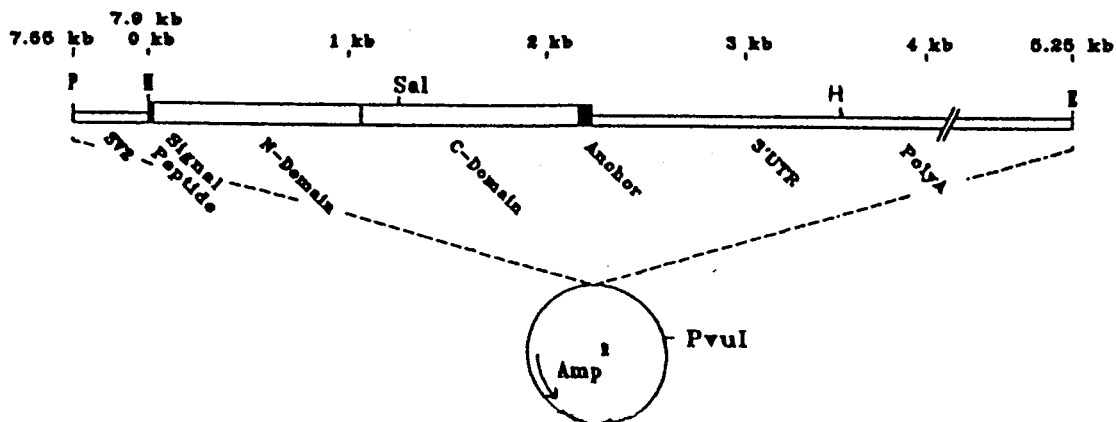
Cell surface biotinylation, PI-PLC treatment, and immunoprecipitation:

Surface proteins of 3.0 x 10⁶ cells were labelled with 0.2 mg biotin (Sigma) as described (53). The cells were washed several times in DMEM, divided into two samples that were incubated for 60 min at 6°C in the presence or absence of PI-PLC (1.7 U/10⁶ cells) respectively. Both the cell supernatant and the cell pellet were subsequently processed. The cells were washed once more and lysed in 50 mM Tris-HCl pH 7.4, 150 mM NaCl, 2 mM EDTA, 0.5% NP-40, 1 mM PMSF and 100 µg/ml lysine to block the excess of free biotin. The same buffer was added to the supernatant. The samples were centrifuged at 12,000 g for 10 min at 4°C to remove the cell nuclei and cell debris. The samples were precleared for 2 h with washed protein A-agarose. The p97 was immunoprecipitated with MAb L235 followed by protein A-agarose precoated with rabbit anti-mouse IgG (Jackson ImmunoResearch). After immunoprecipitation, the beads were washed 6 times in 50 mM Tris-HCl pH 6.5, 150 mM NaCl, 2 mM EDTA, and 0.5% NP-40. The proteins were eluted from the beads in SDS-PAGE loading buffer and separated on an 8% SDS-PAGE gel under reducing conditions. The proteins were transferred onto Immobilon membranes (Millipore) by electroblotting, and detected using peroxidase-conjugated streptavidin (Jackson ImmunoResearch) and the chemiluminescence ECL Western blotting detection system (Amersham) using the conditions recommended by the manufacturer.

Biosynthetic labelling with [³H]-ethanolamine:

The cell line monolayers were biosynthetically labelled for 24 h with [³H] ethan-1-ol-2-amine hydrochloride (20 µCi/ml, 30.4 Ci/mmol, Amersham) in DMEM containing 5% dialyzed FBS, 20 mM HEPES, 100 U/ml penicillin, 100 µg/ml streptomycin, 2 mM L-glutamine, and 50 µM 2-mercaptoethanol. The cells were washed in PBS and lysed in 50 mM Tris-HCl

pH 7.2, 150 mM NaCl, 2 mM EDTA and 0.5% NP-40 with 40 µg/ml PMSF. The lysates were then cleared by centrifugation prior to the immunoprecipitation. The primary antibodies used were the L235 for p97 and the OKT9 for the human TR. Protein A-agarose (BioRad) coated with rabbit anti-mouse IgG antibody (Jackson ImmunoResearch) was added to the samples and incubated for 8 h at 4°C. The resulting complex was washed in 50 mM Tris-HCl pH 6.5, 150 mM NaCl, 2 mM EDTA, and 0.5% NP-40 and resuspended into SDS-PAGE loading buffer. The samples were electrophoresed under reducing conditions on a 10-15% gradient SDS-PAGE gel. After fixation the gel was treated with Amplify (Amersham), dried, and autoradiographed.

Effect of BFA treatment on the transport of p97 to the cell surface:

The fungal metabolite BFA was obtained from Dr. F. Tufaro, of the University of British Columbia, in Vancouver. The experiment involved incubating the SK-MEL-28 cells with bacterial PI-PLC (1.7 U/10^6 cells) for 1 h at 37°C and then washing and incubating the cells at 37°C with 5.0 µg/ml BFA in the regular SK-MEL-28 tissue culture media. The cells were removed after 0, 20 and 40 h, and then were stained with the appropriate primary and fluoresceinated secondary antibodies, and then were washed, fixed and analyzed by FACS for cell surface p97 expression.

Expression of p97 on human tumor lines in a PI-PLC sensitive form:

The human duodenal adenocarcinoma line HuTu-80 (HTB-40) and the human colonic adenocarcinoma line CaCo-2 (HTB-37) were also obtained from the ATCC. These lines were maintained in minimum essential media (MEM) with Earl's balanced salt solution supplemented with 20% FBS, 20 mM HEPES, 100 U/ml penicillin, 100 µg/ml streptomycin, 2 mM L-glutamine, and 0.1 mM non-essential amino acids. The cell lines were

screened by a panel of MAb and the results were visualized by FACS. The sensitivity of the p97 to release by PI-PLC was then determined by FACS.

RESULTS:

Antibodies and Enzymes:

The MAbs used in this work are summarized in Table I. The reactivity of these MAbs with various human and mouse surface antigens are presented in Figures 3 to 5. By comparing Figure 3 (SK-MEL-28) with Figure 4 (p97aTRVBc3), it was apparent that there were four different MAb available which reacted with p97. The MAbs 96.5 and 133.2 were not available for large scale use, thus only the L235 and C MAb were considered for this study. It is interesting to note that the MAb A was extremely reactive to the SK-MEL-28 cells, but not to the p97aTRVBc3 cells, indicating that it was specific for a melanoma associated antigen that was distinct from p97. In Figure 5 it is shown that the anti-mouse MAbs are specific for the mouse antigens and that the anti-human MAbs show no cross reactivity with the mouse antigens. The reverse is the case in Figure 3, where the anti-human MAbs are specific for the human antigens, while the anti-mouse MAbs show no cross reactivity with the human antigens.

The purified MAbs were titrated against the culture supernatants in Figures 6 to 8. In Figure 6 the purified L235 MAb is shown to react reasonably well to p97. The same is not the case for the C MAb, where it appeared that the activity of the purified MAb is somehow impaired by the purification procedure (Figure 7). For this reason the L235 MAb was chosen to be the anti-p97 MAb for this study. The titration of the anti-TR MAb, OKT9 provided an interesting result (Figure 8). The use of serum free tissue culture media instead of serum containing media did not impair the ability of the hybridoma cells to produce active MAbs. In the future this media will be used to produce MAbs in our laboratory.

Table I: Summary of the properties of the MAbs used in this study.

Unless otherwise stated the MAb culture supernatants were used at 100 μl for 10^6 cells.

Antigen	Name	Species	Type	Source	Supply
Human HLA A2/28	PA 2.1	Mouse	IgG	ATCC	Supernatant
Human FNR	FNR	Rabbit	Antisera	Telios	Purified
Human Melanoma	A	Mouse	IgG	Liao	Supernatant
Human p97	96.5	Mouse	IgG2a	Hellström	Purified
Human p97	133.2	Mouse	IgG2a	Hellström	Purified
Human p97	L235	Mouse	IgG1	ATCC	Both
Human p97	C	Mouse	IgG	Liao	Both
Human TR	OKT9	Mouse	IgG1	ATCC	Both
Mouse H-2b	20-8-4s	Mouse	IgG2a	ATCC	Supernatant
Mouse Thy-1	T24/37.1	rat	IgG1	Hyman	Supernatant
Mouse TR	∂E1/9.9.3	rat	IgG1	Takei	Supernatant

Figure 3: Reactivity of various MAbs with surface antigens of SK-MEL-28 cells.

The cell surface antigens were labelled with the primary and the appropriate fluoresceinated secondary antibody. After washing and fixing, the samples were analyzed by FACS. The results were converted to linear scale and normalized with respect to unstained negative control samples.

SK-MEL-28
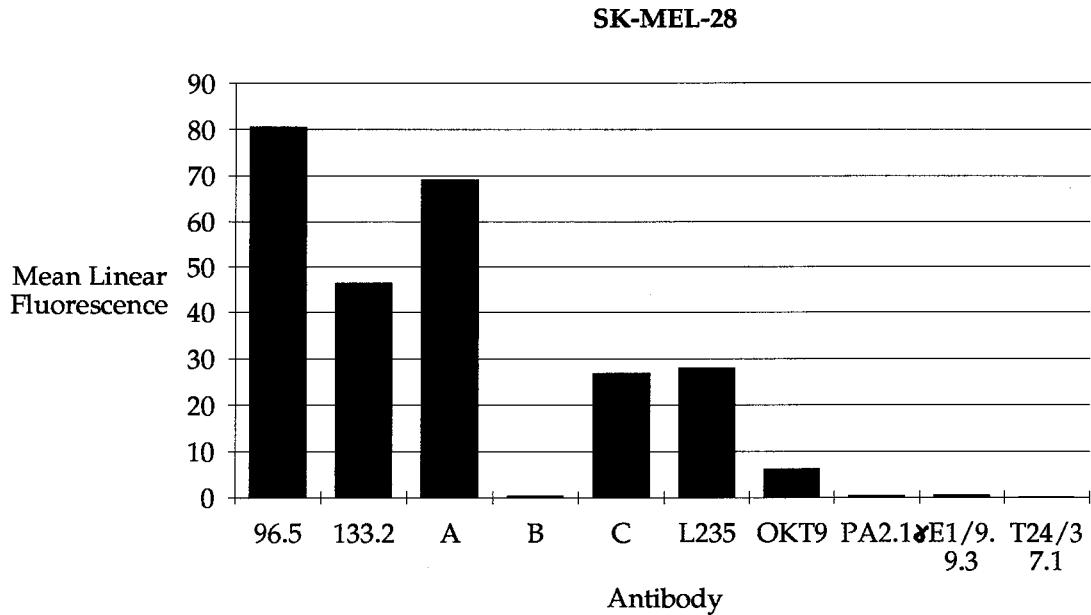
Figure 4: Reactivity of various MAbs with surface antigens of p97aTRVBc3 cells.

The cell surface antigens were labelled with the primary and the appropriate fluoresceinated secondary antibody. After washing and fixing, the samples were analyzed by FACS. The results were converted to linear scale and normalized with respect to unstained negative control samples.
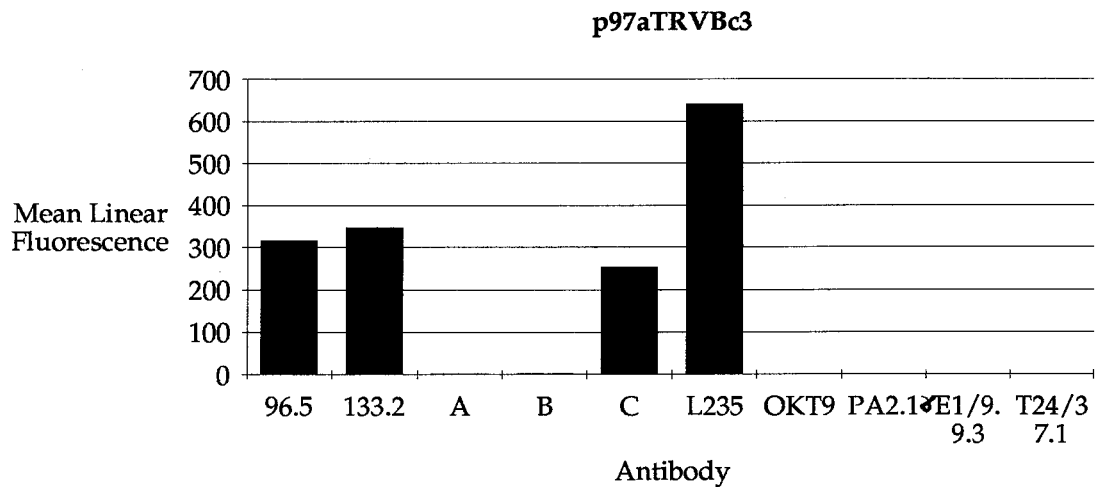
Figure 5: Reactivity of various MAbs with surface antigens of EL-4 cells.

The cell surface antigens were labelled with the primary and the appropriate fluoresceinated secondary antibody. After washing and fixing, the samples were analyzed by FACS. The results were converted to linear scale and normalized with respect to unstained negative control samples.

EL-4
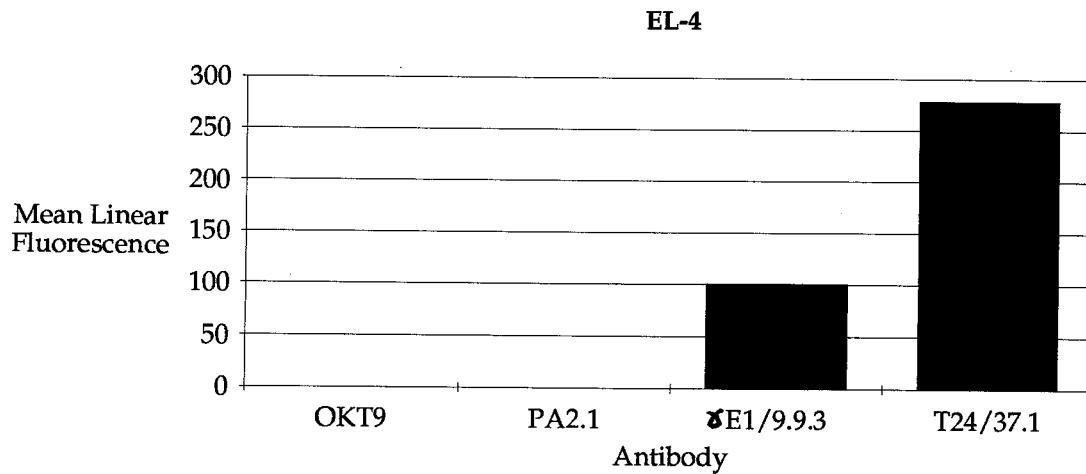
Figure 6: Titration of purified L235 MAb reactivity against SK-MEL-28 cells.

Tissue culture supernatants of the L235 MAb were centrifuged and filtered. The MAb was then purified with a protein G column (Pharmacia). The MAb was then diluted in FACS buffer and incubated with SK-MEL-28 cells. The appropriate fluoresceinated secondary antibody was then used. After washing and fixing, the samples were analyzed by FACS. The results were converted to linear scale and normalized with respect to unstained negative control samples.

L235
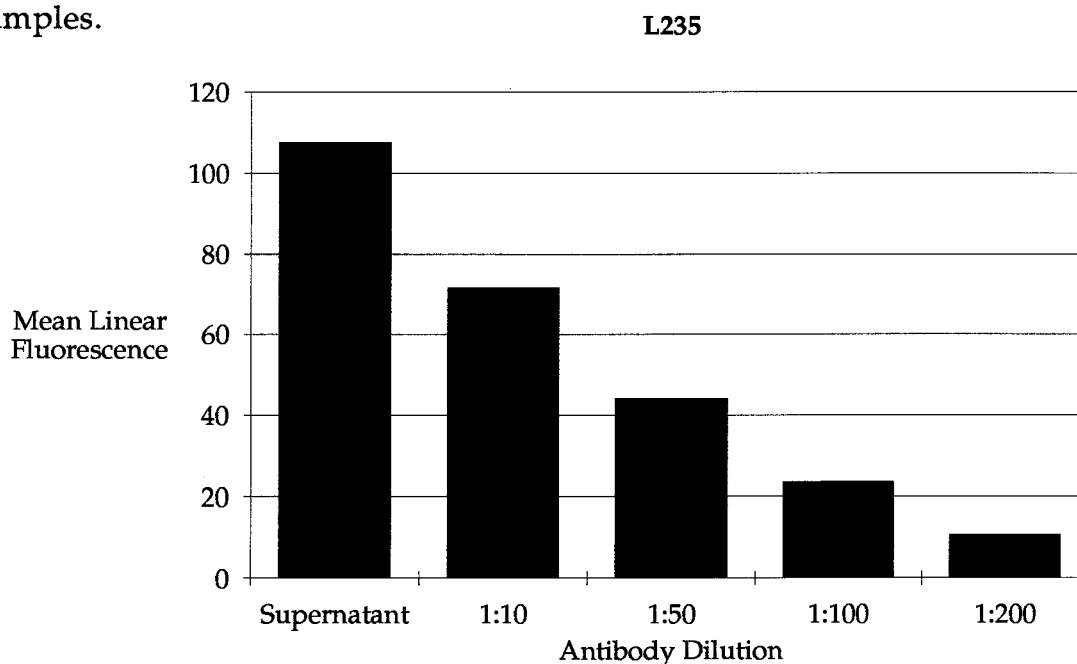
Figure 7: Titration of purified C MAb reactivity against SK-MEL-28 cells.

Tissue culture supernatants of the C MAb were centrifuged and filtered. The MAb was then purified with a protein G column (Pharmacia). The MAb was then diluted in FACS buffer and incubated with SK-MEL-28 cells. The appropriate fluoresceinated secondary antibody was then used. After washing and fixing, the samples were analyzed by FACS. The results were converted to linear scale and normalized with respect to unstained negative control samples.

C

Figure 8: Titration of purified OKT9 MAb reactivity against HuTu-80 cells.

Tissue culture supernatants of the OKT9 MAb were centrifuged and filtered. The MAb was then purified with a protein G column (Pharmacia). The MAb was then diluted in FACS buffer and incubated with HuTu-80 cells. The appropriate fluoresceinated secondary antibody was then used. After washing and fixing, the samples were analyzed by FACS. The results were converted to linear scale and normalized with respect to unstained negative control samples.
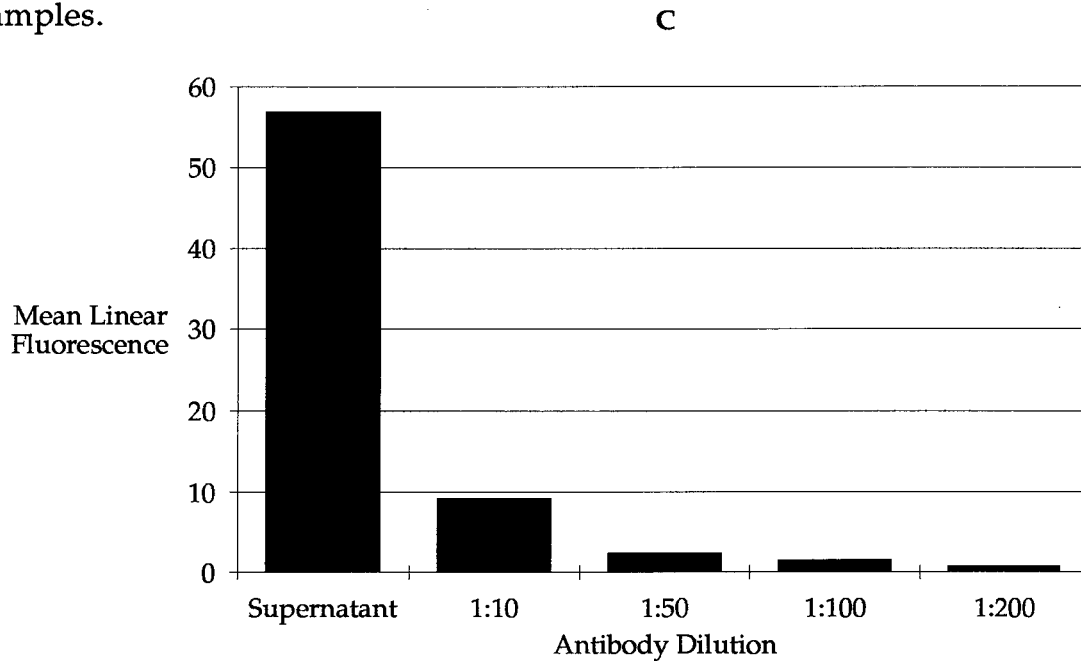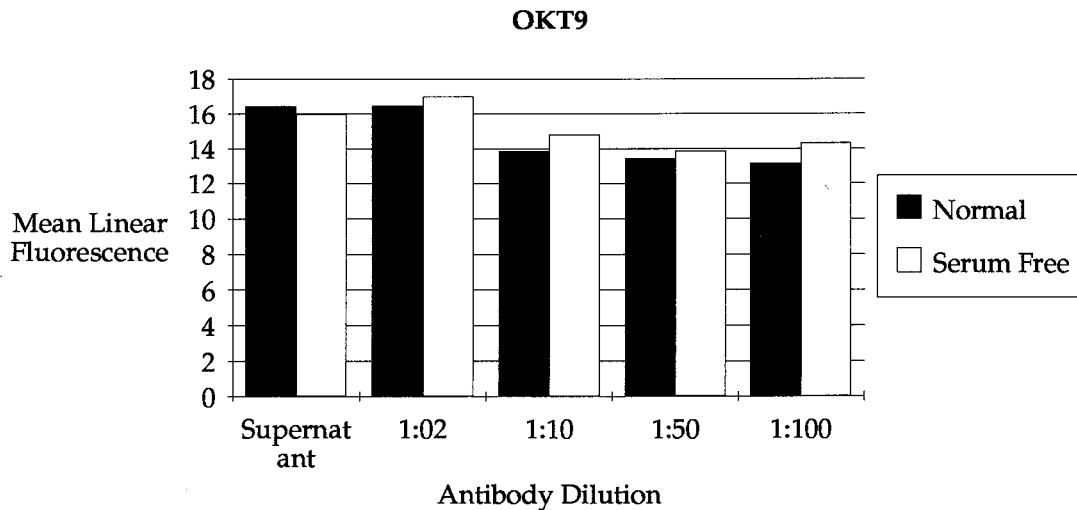
OKT9

The effects of the various PI-PLC preparations and pronase on the human and mouse cell surface antigens of interest were investigated (Table II). While the crude and pure PI-PLC produced similar results, it was clear that the pure PI-PLC did not affect the TR as much as the crude PI-PLC did. This was perhaps due to contamination of the crude PI-PLC preparation with non-specific proteases from the recombinant *Bacillus subtilis* which was used to produce the PI-PLC. The purified PI-PLC preparation was selected for use in this work, due to the apparent lack of contamination with proteases, and is referred to as simply PI-PLC in subsequent text, Tables and Figures.

Release of p97 by bacterial PI-PLC:

Studies have shown that bacterial PI-PLC can cleave GPI-anchors and release the proteins in a soluble form from intact cells. This cleavage is the most common criterion used in GPI-anchor identification (38). The sensitivity of p97 to treatment with purified bacterial PI-PLC was tested by staining SK-MEL-28 cells with the L235 MAb and measuring the surface expression of p97 by flow cytometry. The release of p97 by bacterial PI-PLC treatment is represented by the profiles in Figure 9. The results were converted from logarithmic to linear scale and are expressed as a percentage of the control (Table III). These values indicate that the amount of p97 expression on SK-MEL-28 cells was decreased to 10% of initial levels by treatment with bacterial PI-PLC. In contrast, the expression of the human TR on SK-MEL-28 cells was not at all changed by treatment with bacterial PI-PLC. An example of a protein known to be GPI-anchored is Thy-1, the mouse lymphocyte antigen (56). The release of Thy-1 by bacterial PI-PLC treatment is also represented by the profiles in Figure 9, and summarized in Table III. The expression of Thy-1 on the EL-4 cells was reduced to 30% of initial levels by

Table II: Effect of various PI-PLC preparations and pronase on human and mouse cell surface antigens.

Cells were incubated for 1 h at 37°C in the appropriate enzyme preparation. The human p97 was labelled with the L235 MAb, the human TR was labelled with the OKT9 MAb, and the human fibronectin receptor was labelled with the antisera from Telios. The mouse Thy-1 was labelled with the T24/37.1 MAb, the mouse TR was labelled wih the γE1/9.9.3 MAb, and the mouse H-2^b was labelled with the 20-8-4s MAb. The appropriate fluoresceinated secondary antibodies were then used. After washing and fixing, the samples were analyzed by FACS. The results were converted to linear scale and normalized with respect to unstained negative control samples and the values expressed as percentages of untreated positive control samples.

Enzyme Treatment	Fluorescence Intensity (% of control)					
	Human			Mouse		
	p97	TR	FNR	Thy-1	TR	H-2b
Crude PI-PLC	22	89.5	101	22	77	93
Pure PI-PLC	2	90	101	21	98	95
Pronase	72	1	190	115	1	92

Figure 9: Effect of bacterial PI-PLC on cell surface antigens.

SK-MEL-28 cells were treated with (c,f), and without (b,e), bacterial PI-PLC. The cells were then labelled for human p97 with the L235 MAb (b,c), and for human TR with the OKT9 MAb (e,f). The negative controls (a,d) were no first antibody stainings of SK-MEL-28 cells which were not treated with bacterial PI-PLC. EL-4 cells were treated with (i,l), and without (h,k), bacterial PI-PLC. The cells were then labelled for mouse Thy-1 with the T24/37.1 MAb (h,i), and for the mouse TR with the γE1/9.9.3 MAb (k,l). The negative controls (g,j) were no first antibody stainings of EL-4 cells which were not treated with bacterial PI-PLC. After incubations with the appropriate fluoresceinated secondary antibodies, the cells were washed, fixed and analyzed by FACS. The log scale profiles are presented in this figure.

Log of Fluorescence Intensity
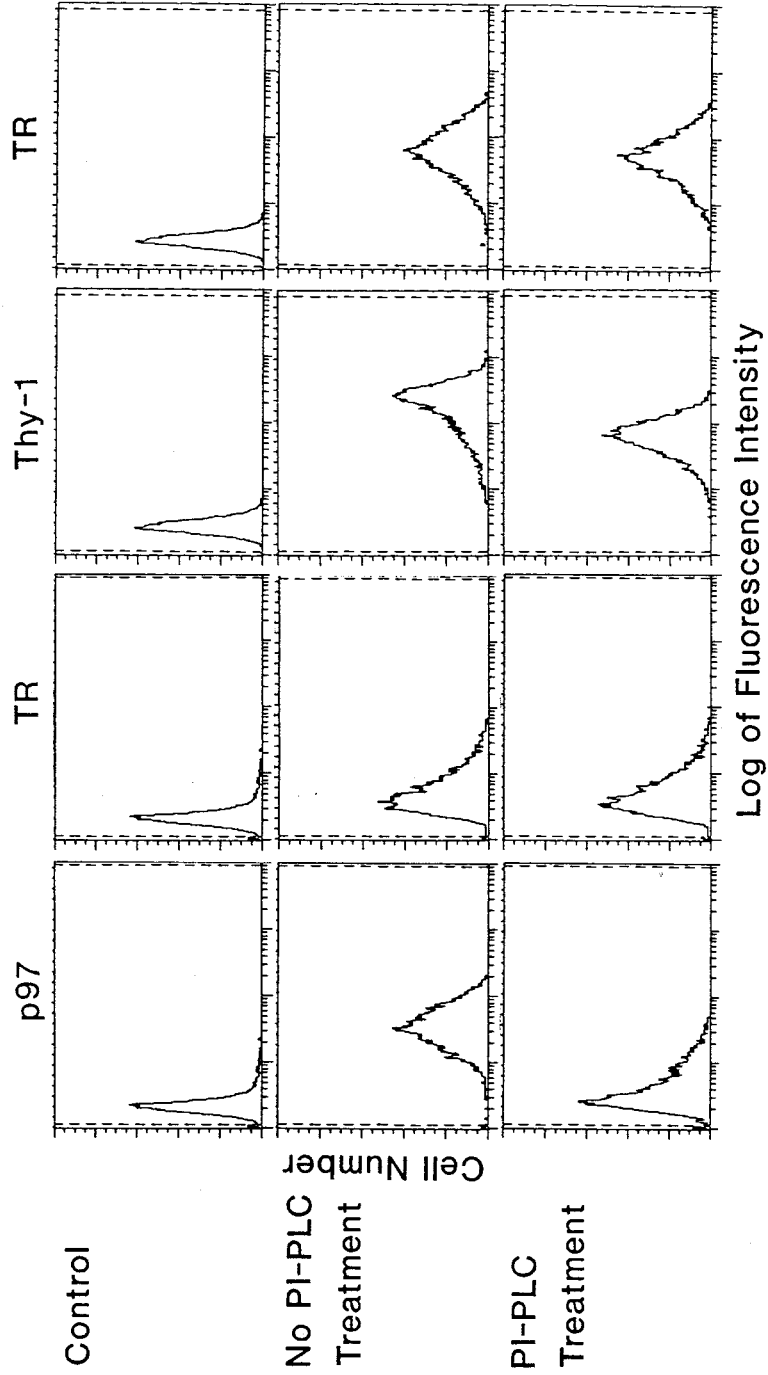
Table III: Effect of bacterial PI-PLC and pronase on human and mouse cell surface antigens.

Cells were incubated for 1 h at 37°C in FACS buffer and 17 U/ml PI-PLC or 1 mg/ml pronase. The human p97 was labelled with the L235 MAb and the human TR was labelled with the OKT9 MAb. The mouse Thy-1 was labelled with the T24/37.1 MAb while the mouse TR was labelled with the γE1/9.9.3 MAb. The appropriate fluoresceinated secondary antibodies were then used. After washing and fixing, the samples were analyzed by FACS. The results were converted to linear scale and normalized with respect to unstained negative control samples and the values expressed as percentages ($\pm$s.d.) of untreated positive control samples. The data presented here are the result of five independent experiments.

Antigen	Cells	Treatment	Fluorescence Intensity (% of control)
p97	SK-MEL-28	PI-PLC	10.8±2.6
p97	SK-MEL-28	Pronase	82.6±17.7
TR	SK-MEL-28	PI-PLC	120.5±16.2
TR	SK-MEL-28	Pronase	15.9±10.8
Thy-1	EL-4	PI-PLC	32.5±6.4
Thy-1	EL-4	Pronase	136.4±20.2
TR	EL-4	PI-PLC	93.1±9.4
TR	EL-4	Pronase	1.9±1.0

treatment with the bacterial PI-PLC, while the expression of the mouse TR on the EL-4 cells was not changed by the bacterial PI-PLC treatment.

To further support the conclusion that the bacterial PI-PLC preparation does not contain a non-specific protease activity, pronase was used to treat cells which were then stained for either the human (p97 or TR) or the mouse (Thy-1 or TR) antigens. The human TR was sensitive to the effects of this enzyme, while p97 was relatively insensitive (Table III). The Thy-1 molecule was PI-PLC sensitive and pronase resistant on the mouse lymphoma line EL-4, while the mouse TR was pronase sensitive and PI-PLC resistant (Table III). The results of these control experiments are in agreement with published data (56).

Partitioning in Triton X-114:

The technique of phase separation in Triton X-114 can be used to assess the amphipathic or hydrophilic character of a protein and is especially useful to identify GPI-anchored proteins (38). This technique is based on the ability of the detergent Triton X-114 to partition into two phases: a detergent rich phase and a detergent poor phase. Amphipathic proteins which possess a hydrophobic membrane anchor primarily partition into the detergent rich phase, whereas hydrophilic proteins partition into the aqueous phase. Proteins with intact GPI-anchors will also partition into the detergent rich phase.

In order to investigate p97 partitioning in Triton X-114, the cell surface proteins were labelled with biotin, washed, and incubated in the presence or absence of bacterial PI-PLC. Both the cell supernatant and the cell pellet were processed for phase separation. The p97 and TR were immunoprecipitated by MAb L235 and OKT9, respectively, followed by Protein A-agarose. The proteins were transferred onto a membrane by electroblotting and detected

Figure 10: Phase separation of p97 and TR in Triton X-114 solution.

SK-MEL-28 cell surface proteins were labelled with biotin. The cells were subsequently washed in DMEM and incubated in the presence (+) or absence (–) of PI-PLC (1.7 U/10^6cells) for 1 h at 6°C. Proteins from the cell pellet (P) or the cell supernatant (S) were separated in Triton X-114 solution, and p97 and TR were immunoprecipitated from both the aqueous phase (A) or the detergent phase (D), as described in the Materials and Methods.

using peroxidase conjugated streptavidin and the chemiluminescence ECL Western blotting detection system. Figure 10 shows that all p97 molecules expressed at the surface of untreated human melanoma SK-MEL-28 cells partition into the detergent-rich phase. No p97 was detected in the supernatants of untreated cells. Treatment with bacterial PI-PLC led to the partitioning of p97 into the aqueous phase of the cell supernatant sample, indicating that the protein was cleaved from the plasma membrane and released as a hydrophilic form. No p97 could be detected in the bacterial PI-PLC treated cell pellet, indicating that most molecules were bacterial PI-PLC sensitive and that p97 is not simultaneously expressed in a transmembrane and GPI-anchored form at the cell surface. In contrast to p97, the TR, which is inserted in the membrane through a hydrophobic peptide segment, is not affected by bacterial PI-PLC. The amphiphilic structure causes the protein to partition in both phases after separation.

Construction of transfectant cell lines expressing human p97 and sensitivity of p97 to release by bacterial PI-PLC:

In order to examine whether the processing signals for GPI-anchor attachment reside in the p97 sequence, and to demonstrate clearly the specificity of the L235 MAb used in this study, the p97 cDNA was transfected into the CHO lines WTB and TRVB. After sub-cloning by limiting dilution, four lines (p97aWTBc3, p97aWTBc7, p97aTRVBc3, p97aTRVBc6) which stably express p97 were isolated. The development of these cell lines from the parental CHO lines is summarized by the FACS profiles in Figures 11 and 12. The treatment of these lines expressing human p97 with bacterial PI-PLC resulted in a decrease in p97 expression at the cell surface (Figure 13). The expression of p97 decreased to less than 20% of untreated levels in all four of the transfectant cell lines (Table IV).

36

Figure 11: Summary of the development of the CHO line WTB expressing human p97.

WTB cells were stained for p97 by the L235 MAb (b,d,f,h) and then, after incubation with the appropriate fluoresceinated secondary antibody, the cells were washed, fixed and analyzed by FACS. The negative controls (a,c,e,g) were no first antibody stainings of WTB cells. The log scale profiles are presented in this figure.
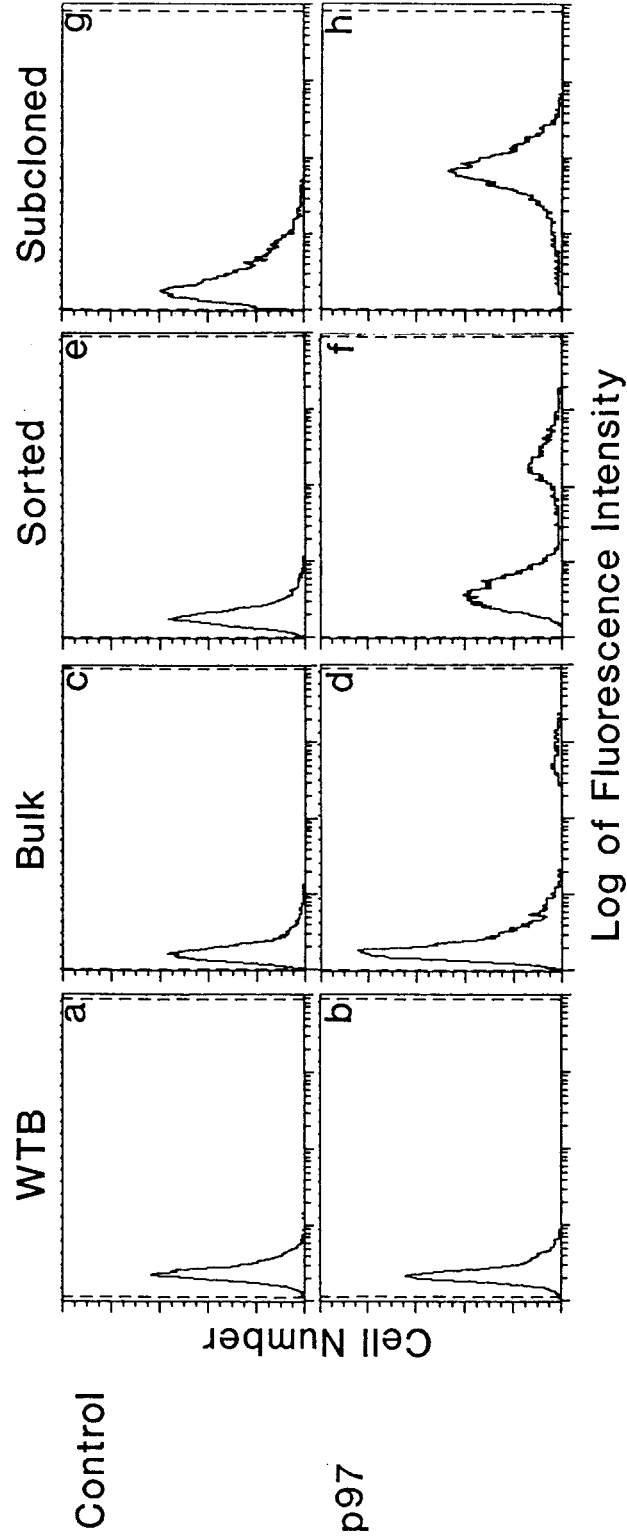
Figure 12: Summary of the development of the CHO line TRVB expressing human p97.

TRVB cells were stained for p97 by the L235 MAb (b,d,f,h) and then, after incubation with the appropriate fluoresceinated secondary antibody, the cells were washed, fixed and analyzed by FACS. The negative controls (a,c,e,g) were no first antibody stainings of TRVB cells. The log scale profiles are presented in this figure.
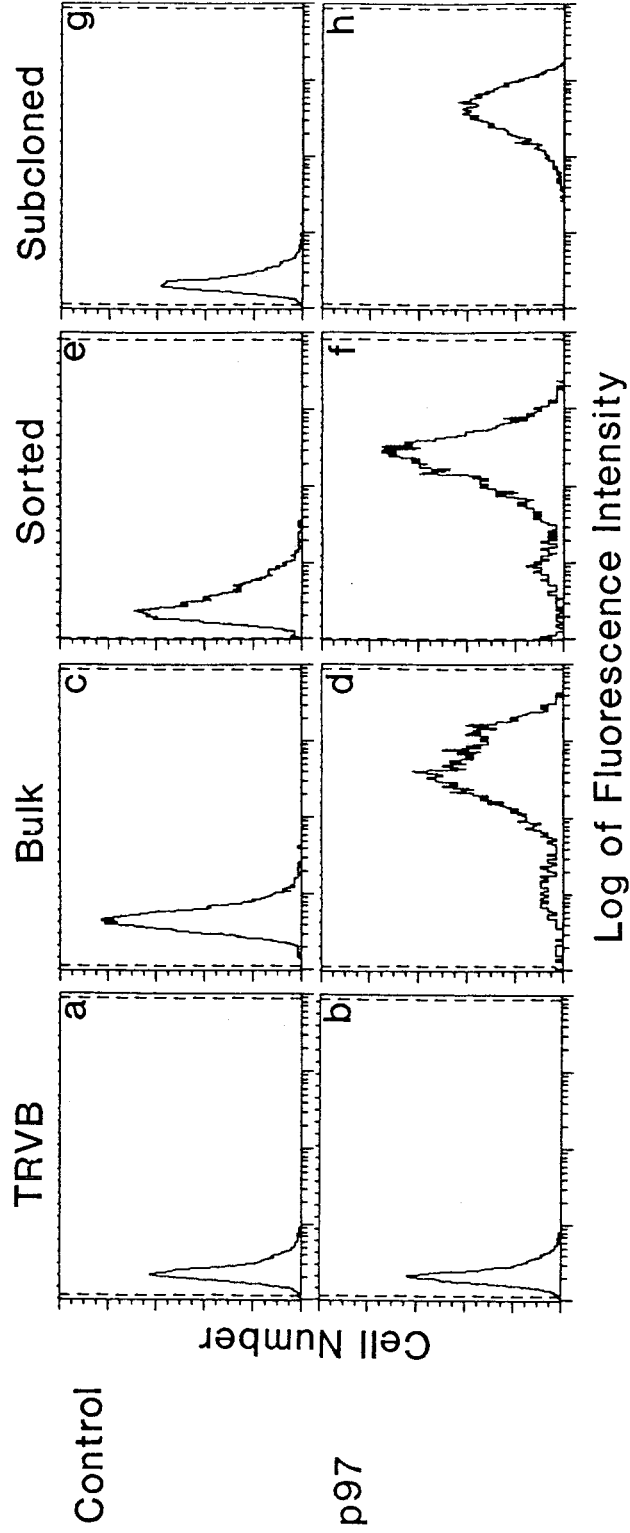
Figure 13: Effect of bacterial PI-PLC on human p97 expressed on the cell surface of various CHO lines.

The transfectant CHO cells were treated with (c,f,i,l), and without (b,e,h,k), bacterial PI-PLC. The cells were then labelled for human p97 with the L235 MAb (b,c,e,f,h,i,k,l). After incubation with the appropriate fluoresceinated secondary antibody, the cells were washed, fixed and analyzed by FACS. The negative controls (a,d,g,j) were no first antibody stainings of the transfectant CHO cells which were not treated with bacterial PI-PLC. The log scale profiles are presented in this figure.
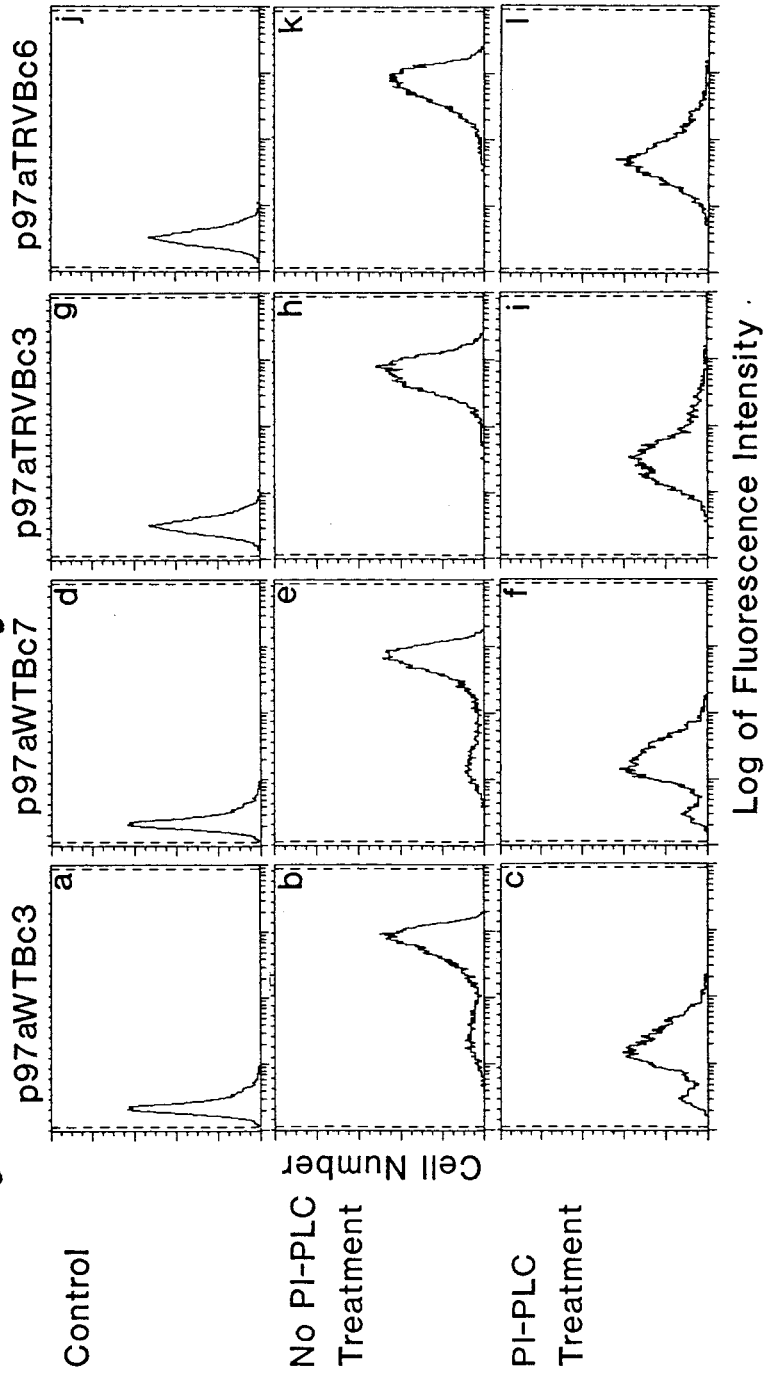
Table IV: Effect of bacterial PI-PLC on human p97 expressed on the cell surface of various CHO lines.

Cells were incubated for 1 h at 37°C in FACS buffer and 17 U/ml PI-PLC. The human p97 was labelled with the L235 MAb. The appropriate fluoresceinated secondary antibody was then used. After washing and fixing, the samples were analyzed by FACS. The results were converted to linear scale and normalized with respect to unstained negative control samples and the values expressed as percentages (±s.d.) of untreated positive control samples. The data presented here are the result of three independent experiments.

Antigen	Cells	Treatment	Fluorescence Intensity (% of control)
p97	p97aWTBc3	PI-PLC	6.8±4.0
p97	p97aWTBc7	PI-PLC	7.5±5.1
p97	p97aTRVBc3	PI-PLC	13.9±4.3
p97	p97aTRVBc6	PI-PLC	19.4±10.3

Figure 14: Effect of bacterial PI-PLC on human p97 expressed on the cell surface of SK-MEL-28 and p97aWTBc7 lines.

Cell surface proteins were labelled with biotin and the cells incubated in the presence (+) or absence (−) of bacterial PI-PLC (1.7 U/10^6 cells) for 1 h at 6°C. Subsequently, p97 was immunoprecipitated from the cell pellets (Panel A) or from the cell supernatants (Panel B) and detected as described in the Materials and Methods. The cell lines analyzed were 1: WTB, 2: p97aWTBc7, 3: SK-MEL-28.
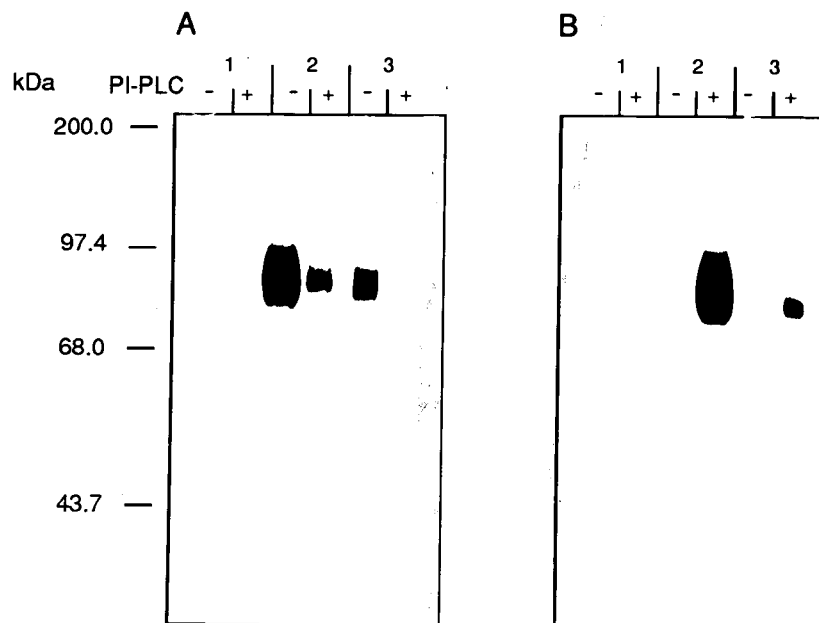
The effect of bacterial PI-PLC and the specificity of the L235 MAb was further characterized in Figure 14 where surface proteins from either WTB, p97aWTBc7 or SK-MEL-28 cells were labelled with biotin and p97 was immunoprecipitated and analyzed on SDS-PAGE under reducing conditions. The proteins were transferred onto a membrane by electroblotting and detected using peroxidase conjugated streptavidin and the chemiluminescence ECL Western blotting detection system. A single protein of 95-97,000 daltons molecular mass was immunoprecipitated from the cell line transfected with the p97 cDNA that was absent in the parental untransfected cell line WTB. The same protein was detected in the human melanoma cell line SK-MEL-28. Treatment of both SK-MEL-28 or the transfected p97aWTBc7 cells with bacterial PI-PLC resulted in a large loss of the protein from the cell surface (Figure 14A). The released protein could be recovered in the cell supernatant (Figure 14B). Under the conditions used in this experiment, no difference in the molecular mass between the plasma membrane associated form and the released form could be detected.

Biosynthetic labelling:

It can not be excluded from the FACS and the biotinylation experiments that the decrease in the expression observed after bacterial PI-PLC treatment is an indirect effect due to the association of p97 with another PI-PLC sensitive protein at the cell surface. To address this issue, the cells in culture were biosynthetically labelled with [^{3}H]-ethanolamine, which is known to be a component of the phospholipid moiety of GPI-anchored proteins (38). The cells were lysed, p97 or TR were immunoprecipitated, and run on SDS-PAGE under reducing conditions. The p97 and TR molecules were immunoprecipitated by the L235 and OKT9 MAbs respectively, in the SK-MEL-28 cell line (Figure 15). The p97 is labelled by the [^{3}H]-ethanolamine

Figure 15: Biosynthetic labelling of p97 with [^{3}H]-ethanolamine in SK-MEL-28 cells.

SK-MEL-28 cell monolayers were biosynthetically labelled in duplicate with [^{3}H]-ethanolamine and proteins were immunoprecipitated with the appropriate MAb. These complexes were separated on a 10-15% SDS-PAGE gel and autoradiographed. In Lanes 1 and 2 p97 was immunoprecipitated with the L235 MAb. The observed difference in labelling intensity may be due to slight differences between the individual plates used in the immunoprecipitation. Lanes 3 and 4 show the immunoprecipitation of the human TR with the OKT9 MAb.
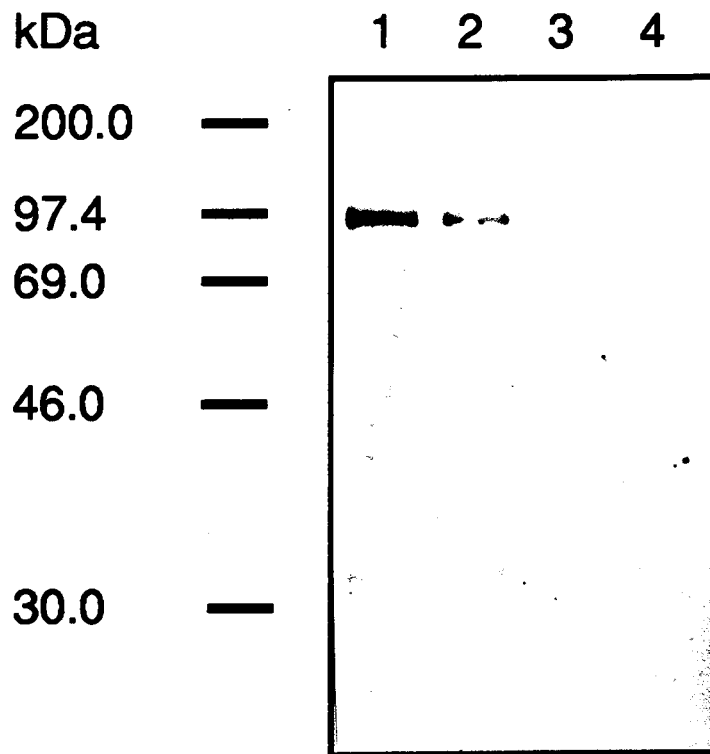
(lanes 1+2) while theTR is not (lanes 3+4). The p97 in both the p97aWTBc3 line (Figure 16: lane 3) and the p97aTRVBc3 (Figure 17: lane 3) line was also labelled by the [^{3}H]-ethanolamine.

Effect of BFA on the transport of p97 to the cell surface:

The effect of the fungal metabolite BFA on the transport of p97 to the cell surface was also investigated. The SK-MEL-28 cells were treated with PI-PLC (1.7 U/10^6 cells) in DMEM and then were allowed to recover in the presence or absence of BFA. It is clear that the 5 µg/ml BFA concentration disrupted the transport of the p97 molecule to the cell surface (Table V). The results of these experiments with regards to the blocking of surface expression of a GPI-anchored protein by BFA are in agreement with previous work on alkaline phosphatase (57).

Expression of p97 on human tumor cell lines in a PI-PLC sensitive form:

The presence of p97 on the cell surface of two different human intestinal tumor lines was investigated using a variety of MAb against p97. The results of these experiments were consistent for both lines in that p97 was expressed at a fairly low level compared to the human TR (Figures 18,19). The effects of bacterial PI-PLC treatment on these antigens are summarized in Table VI. It is again evident that p97 is sensitive to treatment with PI-PLC, while the TR is not sensitive to the effects of this enzyme.

Figure 16: Biosynthetic labelling of p97 with [3H]-ethanolamine in p97aWTBc3 cells.

WTB (Lane 1,2) and p97aWTBc3 (Lane 3,4) cell monolayers were biosynthetically labelled with [3H]-ethanolamine and proteins were immunoprecipitated with the appropriate MAb. The complex was then analyzed as in Figure 14. Lane 3 shows the immunoprecipitation of p97 with L235 MAb. Lanes 1 (L235), 2 (OKT9), and 4 (OKT9) indicate that the MAb used in this experiment do not cross react with labelled hamster antigens.

kDa	1	2	3	4
200.0 —				
97.4 —			▬	
69.0 —				
46.0 —				
30.0 —				

Figure 17: Biosynthetic labelling of p97 with [^{3}H]-ethanolamine in p97aTRVBc3 cells.

TRVB (Lane 1,2) and p97aTRVBc3 (Lane 3,4) cell monolayers were biosynthetically labelled with [^{3}H]-ethanolamine and proteins were immunoprecipitated with the appropriate MAb. The complex was then analyzed as in Figures 14 and 15. Lane 3 shows the immunoprecipitation of p97 with L235 MAb. Lanes 1 (L235), 2 (OKT9), and 4 (OKT9) indicate that the MAb used in this experiment do not cross react with labelled hamster antigens.
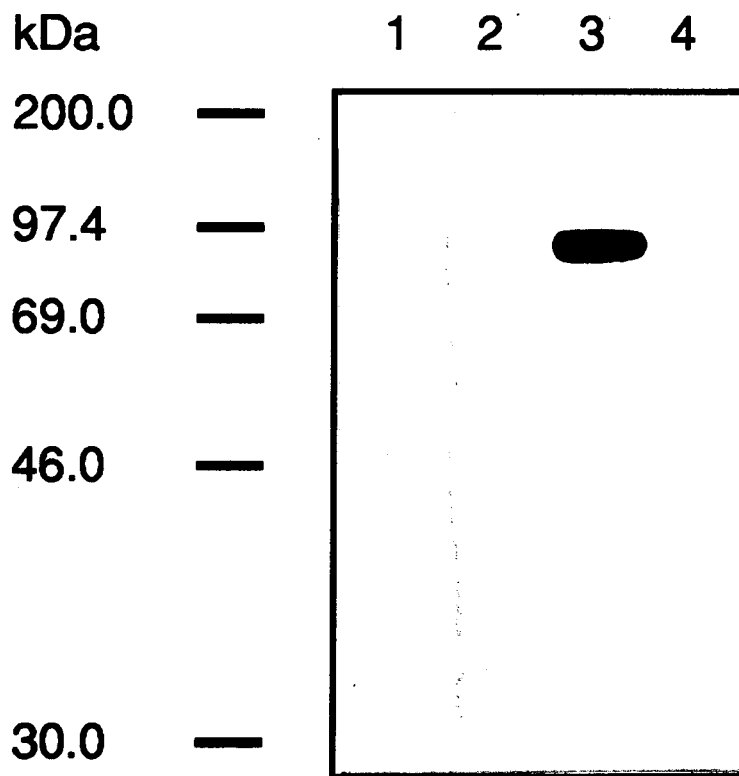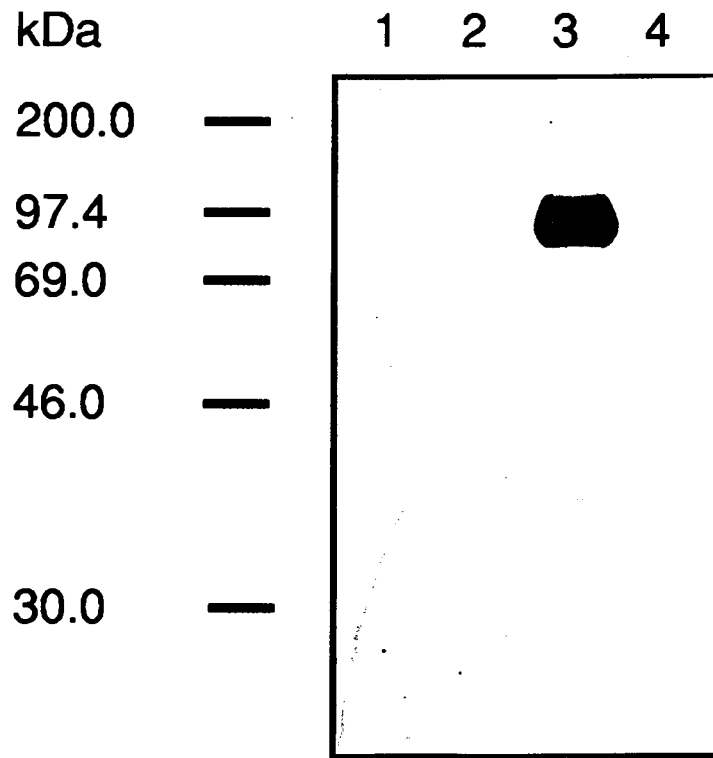
Table V: Effect of BFA on the transport of p97 to the surface of SK-MEL-28 cells.

SK-MEL-28 cells which had been treated with 17 U/ml PI-PLC for one h at 37°C were then allowed to recover at 37°C with 5.0 µg/ml BFA in DMEM or DMEM alone. At various times (0, 20, 40 h) cells were removed and incubated with the L235 MAb. After incubation with the appropriate fluoresceinated secondary antibody, the cells were washed, fixed, and analyzed by FACS. The results were converted to linear scale and normalized with respect to unstained negative control samples, and the values expressed as percentages of untreated positive control samples.

Treatment Initial	Treatment Recovery	Time (h)	% of p97 remaining on cell surface
No	No	0	100.00
No	No	20	100.00
No	No	40	100.00
PI-PLC	No	0	2.30
PI-PLC	No	20	8.81
PI-PLC	No	40	52.80
PI-PLC	BFA	0	2.30
PI-PLC	BFA	20	0.30
PI-PLC	BFA	40	0.00
No	BFA	0	100.00
No	BFA	20	49.83
No	BFA	40	15.00

Figure 18: Reactivity of various MAbs with surface antigens of CaCo-2 cells.

The cell surface antigens were labelled with the primary and the appropriate fluoresceinated secondary antibody. After washing and fixing, the samples were analyzed by FACS. The results were converted to linear scale and normalized with respect to unstained negative control samples.

CaCo-2

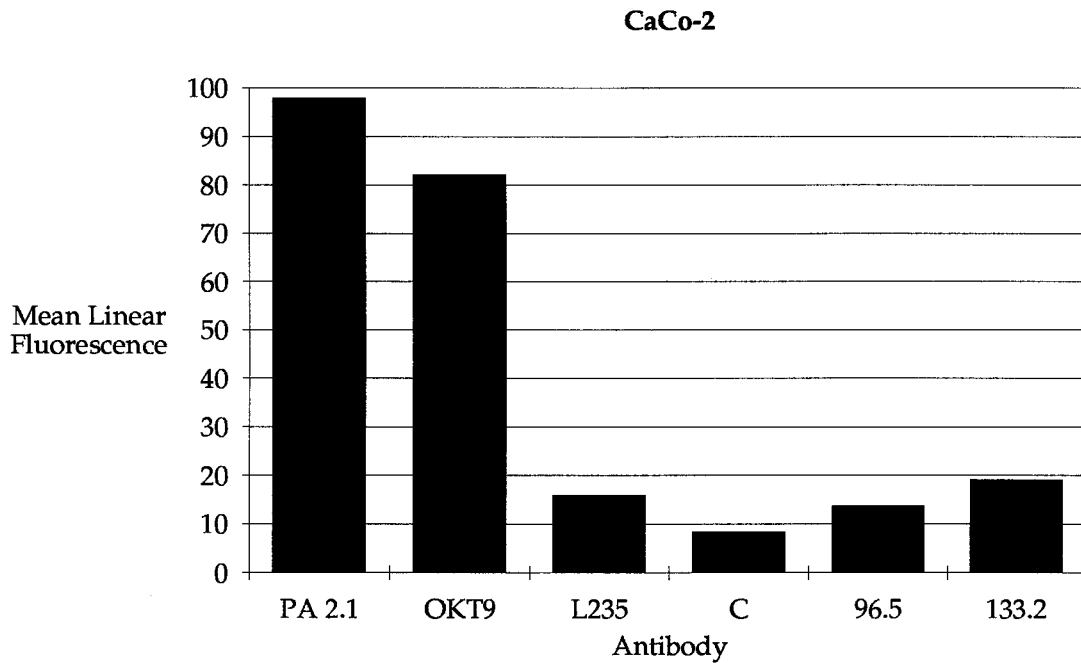Figure 19: Reactivity of various MAbs with surface antigens of HuTu-80 cells.

The cell surface antigens were labelled with the primary and the appropriate fluoresceinated secondary antibody. After washing and fixing, the samples were analyzed by FACS. The results were converted to linear scale and normalized with respect to unstained negative control samples.

HuTu-80
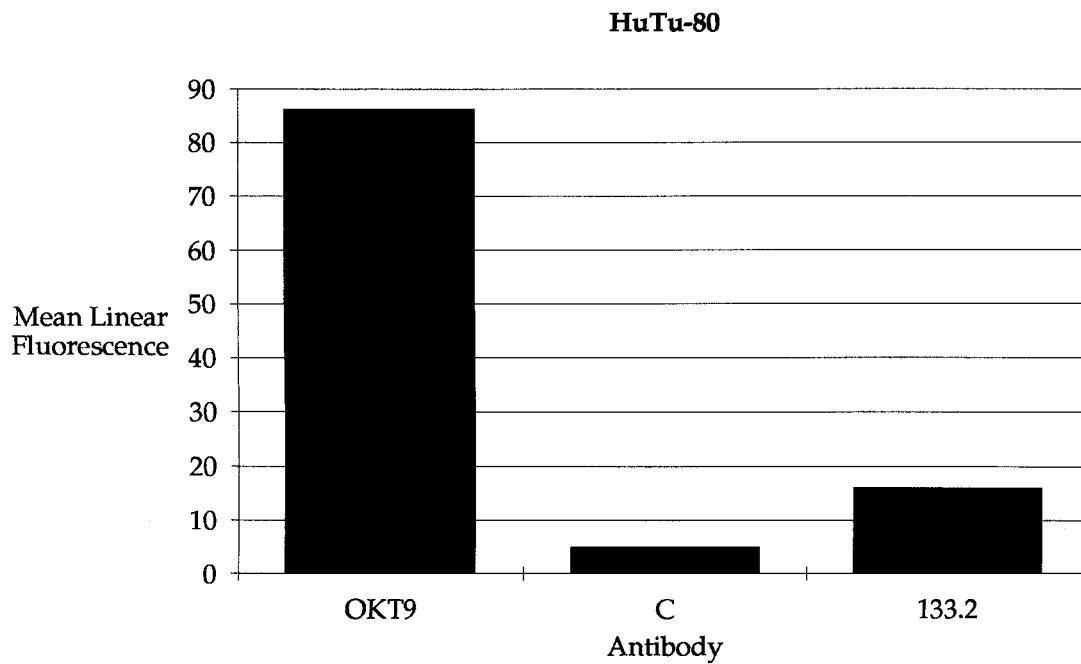
Table VI: Effect of bacterial PI-PLC on human p97 expressed on the cell surface of various human intestinal lines.

Cells were incubated for 1 h at 37°C in FACS buffer and 17 U/ml PI-PLC. The human p97 was labelled with the L235 MAb and the human TR was labelled with the OKT9 MAb. The appropriate fluoresceinated secondary antibodies were then used. After washing and fixing, the samples were analyzed by FACS. The results were converted to linear scale and normalized with respect to unstained negative control samples and the values expressed as percentages (±s.d.) of untreated positive control samples. The data presented here are the result of three independent experiments, with the exception of the HuTu-80 p97 determination which was completed once.

Antigen	Cells	Treatment	Fluorescence Intensity (% of control)
p97	CaCo-2	PI-PLC	35.0±22.4
TR	CaCo-2	PI-PLC	94.0±17.9
p97	HuTu-80	PI-PLC	15.4
TR	HuTu-80	PI-PLC	87.0±8.1

DISCUSSION:

In this work it is shown that p97 is attached to the cell surface via a GPI-anchor. The first section demonstrates that p97 is sensitive to the effects of bacterial PI-PLC. This technique is commonly used to test for the presence of a GPI-anchor. In this case p97 was clearly shown to be sensitive to the effects of purified bacterial PI-PLC in the human melanoma line SK-MEL-28 (Figure 9, Table III). The effect was not due to contaminating protease activity, as was shown by the relative insensitivity of p97 to pronase. The human TR was used as an example of a typical transmembrane protein, which was bacterial PI-PLC resistant and pronase sensitive. The detergent Triton X-114 was used to partition the p97 and TR, a further test for the presence of a GPI-anchor (Figure 10). It is clear from this experiment that p97 possesses a lipid anchor, which permits it to partition in the detergent phase of the pellet after no bacterial PI-PLC treatment, and the aqueous phase of the supernatant after bacterial PI-PLC treatment.

The specificity of MAb L235 for p97, and the presence of the information necessary to confer GPI-anchor attachment in the p97 cDNA, are proven by the transfections of the CHO cells with the p97 cDNA. As well, the machinery responsible for the synthesis of the GPI-anchor, and its attachment to the p97 protein, is shown to be present in the CHO line, in a form that recognizes some signal on the p97 pre-protein. The data for the transfectant cell lines where bacterial PI-PLC release was visualized by FACS (Figure 13, Table IV), by cell surface labelling (Figure 14), and the biosynthetic labelling with [^{3}H]-ethanolamine (Figures 16,17), all indicate that the L235 MAb recognized the protein product of the p97 cDNA. It is also clear from these figures that the expression of p97 by the transfectant lines is considerably greater than for the melanoma line. Since the experiments showed that the

same form of the p97 molecule was present on the transfectant lines as on the melanoma line, it is presumed that this form maintains the properties of the molecule. These lines should, therefore, be useful in the study of the functional aspects of the p97 molecule.

It was also demonstrated by biosynthetic labelling that p97 is not simply associated with a GPI-anchored protein at the cell surface (Figures 15-17). The presence of [^{3}H]-ethanolamine in the p97 from both melanoma and transfected CHO lines indicated that p97 is indeed GPI-anchored. The significance of this GPI-anchor with respect to intracellular transport was investigated with BFA (Table V). It is obvious that the lipid anchor does not enable the p97 molecule to procede to the cell surface via a transport mechanism distinct from the standard protein pathway, as is the case for cholesterol and phosphatidylethanolamine (58,59). To complete the investigation, the presence of p97 in a bacterial PI-PLC sensitive form on two human intestinal carcinoma lines was demonstrated (Figures 18,19 and Table VI).

Unlike Tf, which is a soluble protein whose uptake is mediated by the TR, p97 is expressed at the cell surface. The structure of the GPI-anchor confers important biophysical differences between this and the conventional method of protein anchoring (e.g.: anchor via a protein transmembrane hydrophobic region), therefore, the finding that p97 is GPI-anchored has several consequences. A major feature of GPI-anchored proteins which distinguishes them from other membrane proteins is their ability to be released from membranes by the action of bacterial PI-PLC. The identification of mammalian GPI-anchor hydrolysing enzymes (48) suggests that one function of the anchor might be to allow the rapid release of the protein. The GPI-anchor could provide a very specific way for a cell to regulate the

expression of p97 at the cell surface at a post-translational level, using the anchor as a quick release method of down regulation at the cell surface, or up regulation of the protein in circulation (39). In fact, the GPI-anchor of p97 may be present to allow the cell to release a soluble form of p97 in response to a cue or signal. The existence of soluble p97 in the spent tissue culture medium of human melanoma cells has been previously documented (29). We have also detected a water soluble form of the p97 protein in tissue culture medium, and the source from which this form of the p97 molecule originates is currently under investigation (data not shown).

A further consequence of lipid anchoring is an inherent increase in lateral mobility in the plane of the membrane and exclusion from coated pits involved in receptor mediated endocytosis (38). It has been shown that the GPI-anchored folate receptor is excluded from the clathrin coated pits, but associates with small invaginations on the cell surface termed caveolae, which are capable of mediating the internalization of its ligand (60-62). It has also been shown that a GPI-anchored form of CD4 is internalized by a mechanism which is different from that of the folate receptor in that the receptors are clearly internalized in vesicles (45). It is possible that p97 could be directly involved in iron uptake in melanoma cells. While cellular iron uptake has been shown to be mediated mainly by the Tf/TR pathway, there is evidence for a non-Tf mediated pathway of iron incorporation in various cell lines (12-15). Since iron is an absolute requirement for cell growth, there are several potential consequences of a p97 mediated iron uptake system in terms of the development of melanoma. Melanoma cells may have a growth advantage over normal cells by combining two iron uptake pathways, one which is mediated by TR and the other which is mediated by p97.

Alternatively, p97 could deprive normal cells surrounding the tumor of their iron supply, resulting in cell death and the further expansion of the tumor.

The potential iron uptake capacity of p97 has been investigated. It was suggested that p97 was responsible for an iron uptake activity evident in SK-MEL-28 cells (16). In a subsequent report by the same group (17), it was stated that p97 was not contributing to iron utilized by the cell. The next report from this group concluded that p97 was not involved in the uptake of iron from inorganic complexes (18). The most recent report from this group investigated the effect of ferric ammonium citrate and desferrioxamine on the uptake of iron by the SK-MEL-28 cells (19). It is suggested that the iron uptake evident is due to the processes described previously (16). This group have not yet demonstrated that the non-Tf bound membrane iron uptake activity is due to the action of p97. An experiment which might address this problem is to examine the activity of this non-Tf bound membrane uptake system after treatment with bacterial PI-PLC. Presumably, if p97 was responsible for the observed activity, the iron uptake activity would be abolished by the bacterial PI-PLC treatment. One further problem which is apparent in these papers is that the iron uptake component which is attributed to p97 is stated to be pronase sensitive (16). The data presented in this work indicate that p97 is relatively insensitive to the effects of pronase. If both sets of data are correct, one possible explanation for this situation is that the activity which they attribute to p97 is not due to p97, but some other non-Tf membrane iron uptake system.

The original description of the iron binding capacity of p97 was done on SK-MEL-28 cells which were incubated with [^{59}Fe] as $FeCl_3$, and then cell lysates were exposed to various MAb and the mixture was passed over a column (25). While it was clear that p97 could bind iron, the number of

atoms of iron bound per molecule of p97 was not known. It was recently suggested that only one functional iron-binding site exists on the p97 molecule (63). It is thought that the iron binding properties of the N-terminal site of p97 are conserved, but those of the C-terminal site are not (63). Since the purification scheme used in this experiment appears to isolate only the membrane bound form of p97, perhaps the result is only applicable to the GPI-anchored form of p97 and not the soluble form of p97. An interesting study would be to carry out the same iron binding experiment on bacterial PI-PLC released, purified p97. It is possible that the presence of the plasma membrane so close to the C-terminal site is the only factor preventing the interaction of the iron with the binding site (64). Alternatively, the p97 molecule may only require the N-terminal site for whatever function it is involved in (63).

One area of concern in regards to the single atom of iron/p97 molecule hypothesis is the wavelength used to measure the amount of iron bound. The electronic absorption spectrum of iron-saturated human serum Tf has been reported to peak at 464 nm (63) or 473 nm (65). Unfortunately, similar data does not exist for the p97 molecule. The single atom of iron/p97 molecule determination used the λ_{max} of 464 nm (63), while another group has suggested that the λ_{max} of 420 nm is more appropriate for p97 (65). This group worked with site directed mutants of the N-terminal half of human Tf. In one of these mutants (D63S) the aspartic acid (Tf) to serine (p97) switch which is evident when comparing the C-terminal regions of Tf and p97 was put in the N-terminal half of the Tf, and the resulting molecule was investigated. It was found that the λ_{max} of this mutant Tf was 420 nm (65). For this reason, it is not completely convincing that there is only one atom of iron bound to the p97 molecule (R. T. A. MacGillivray, personal

communication). It remains to be seen if p97 has one or two functional iron binding pockets, and if it makes a difference to the function of the molecule.

There is an experiment which can be completed using cell lines produced in this work which might directly address the question of the function of p97. It would involve using the parental CHO line TRVB (66), which expresses no functional TR, and the transfectant CHO lines p97aTRVBc3 and p97aTRVBc6, which express high levels of p97. The experiment would involve incubating samples of both the transfected and untransfected TRVB lines with [^{59}Fe] as $FeCl_3$ and then washing the cells and measuring the amount of iron internalized. If p97 does indeed contribute to the iron uptake capacity of the p97aTRVB lines it would follow that the amount of labelled iron internalized would be far greater than for the parental TRVB line. A useful positive control would be the CHO line WTB which expresses functional hamster TR, and should take up the iron by the standard Tf/TR pathway. A further control could be the use of PI-PLC on the p97aTRVB line immediately before the incubation with the labelled iron, which should decrease the amount of iron internalized, if p97 does contribute to iron uptake.

One further consequence of the GPI-anchor of p97 is in the potential cellular distribution of the protein. In polarized epithelial cells, it is known that GPI-anchored proteins can be localized to the apical membrane (67,68). Presumably, if expressed, p97 will be apically distributed in these cells. The CaCo-2 cell line has been used as a model system for studying the transport of iron across epithelial cell monolayers (69). Given that p97 is present in a PI-PLC sensitive form on the surface of the CaCo-2 cells, it is possible that this system could be used to investigate the potential iron uptake capacity of p97. The experiment would involve treating cells with, or without, bacterial PI-

PLC and observing the effect on iron uptake. If the expression of p97 was too small to make a serious contribution to the measurable iron uptake, it would be possible to transfect the CaCo-2 cells with the p97 cDNA in the same manner as the CHO lines were in this work, to make a system which might better demonstrate the effect. This experiment could extend the work with the iron uptake in the p97aTRVB cell lines to a more physiological situation.

The final functional implication of the GPI-anchor of p97 is that it may participate in signal transduction. There is evidence that GPI-anchored proteins can be complexed to protein tyrosine kinases, however, it is not known how these GPI-anchored molecules can transduce signals (70). This may be important for the role of p97 in melanomas, and may contribute to cancer progression. It is known that PI turnover is important for vision in *Drosophila* and cell proliferation in some cultured cells (71). Perhaps the most important part of the p97 molecule is the 1,2 diacylglycerol products which result from the reaction catalyzed by PI-PLC, and not the soluble p97 released.

CONCLUDING STATEMENT:

The major finding in this work is that the human melanoma-associated antigen p97 is attached to the plasma membrane via a GPI-anchor. At the present time investigations are being carried out in our laboratory to determine both the distribution and the function of the p97 molecule.

REFERENCES:

1. **Ross, P. M. and D. M. Carter.** 1989. Actinic DNA Damage and the Pathogenesis of Cutaneous Malignant Melanoma
. *J. Invest. Dermatol.* 92:293s.

2. **Council on Scientific Affairs.**, 1989. Harmful Effects of Ultraviolet Radiation. *JAMA 262*:380.

3. **Ananthaswamy, H. N. and W. E. Pierceall.** 1990. Molecular Mechanisms of Ultraviolet Radiation Carcinogenesis. *Photochem. Photobiol. 52*:1119.

4. **Truhan, A. P.** 1991. Sun protection in childhood. *Clin. Pediatr. 30*:676.

5. **Robinson, W. A.** 1990. Malignant melanoma as a model for cancer education and prevention. *J. Cancer Educ. 5*:85.

6. **Kühn, L. C., H. M. Schulman, and P. Ponka.** 1990. Iron-Transferrin Requirements and Transferrin Receptor Expression in Proliferating Cells. In *Iron Transport and Storage.* P. Ponka, H.M. Schulman and R.C. Woodworth, eds. CRC Press, Boca Raton, p. 149.

7. **Crichton, R. R. and M. Charloteaux-Wauters.** 1987. Iron transport and storage. *Eur. J. Biochem. 164*:485.

8. **Crosa, J. H.** 1989. Genetics and Molecular Biology of Siderophore-Mediated Iron Transport in Bacteria. *Microbiol. Rev. 53*:517.

9. **Baker, E. N., S. V. Rumball, and B. F. Anderson.** 1987. Transferrins: insights into structure and function from studies on lactoferrin. *Trends Biochem. Sci.* *12*:350.

10. **Kühn, L. C.** 1989. The transferrin receptor: a key function in iron metabolism. *Schweiz. Med. Wschr. 119*:1319.

11. **Morgan, E. H.** 1981. Transferrin, Biochemistry, Physiology and Clinical Significance. *Molec. Aspects Med.* 4:1.

12. **Basset, P., Y. Quesneau, and J. Zwiller.** 1986. Iron-induced L1210 Cell Growth: Evidence of a Transferrin-independent Iron Transport. *Cancer Res.* *46*:1644.

13. **Sturrock, A., J. Alexander, J. Lamb, C. M. Craven, and J. Kaplan.** 1990. Characterization of a Transferrin-independent Uptake System for Iron in HeLa Cells. *J. Biol. Chem. 265*:3139.

14. **Kaplan, J., I. Jordan, and A. Sturrock.** 1991. Regulation of the Transferrin-independent Iron Transport System in Cultured Cells. *J. Biol. Chem. 266*:2997.

15. **Thorstensen, K.** 1988. Hepatocytes and Reticulocytes Have Different Mechanisms for the Uptake of Iron from Transferrin. *J. Biol. Chem. 263*:16837.

16. **Richardson, D. R. and E. Baker.** 1990. The uptake of iron and transferrin by the human malignant melanoma cell. *Biochim. Biophys. Acta 1053*:1.

17. **Richardson, D. R. and E. Baker.** 1991. The release of iron and transferrin from the human melanoma cell. *Biochim. Biophys. Acta 1091*:294.

18. **Richardson, D. and E. Baker.** 1991. The uptake of inorganic iron complexes by human melanoma cells. *Biochim. Biophys. Acta 1093*:20.

19. **Richardson, D. R. and E. Baker.** 1992. The effect of desferrioxamine and ferric ammonium citrate on the uptake of iron by the membrane iron-binding component of human melanoma cells. *Biochim. Biophys. Acta 1103*:275.

20. **Woodbury, R. G., J. P. Brown, M. Y. Yeh, I. Hellström, and K. E. Hellström.** 1980. Identification of a cell surface protein, p97, in human melanomas and certain other neoplasms. *Proc. Natl. Acad. Sci. USA 77*:2183.

21. **Brown, J. P., R. G. Woodbury, C. E. Hart, I. Hellström, and K. E. Hellström.** 1981. Quantitative analysis of melanoma-associated antigen p97 in normal and neoplastic tissues. *Proc. Natl. Acad. Sci. USA 78*:539.

22. **Woodbury, R. G., J. P. Brown, S. M. Loop, K. E. Hellström, and I. Hellström.** 1981. Analysis of Normal Neoplastic Human Tissues for the Tumor-associated Protein p97. *Int. J. Cancer 27*:145.

23. **Brown, J. P., K. Nishiyama, I. Hellström, and K. E. Hellström.** 1981. Structural Characterization of Human Melanoma-Associated Antigen p97 with Monoclonal Antibodies. *J. Immunol. 127*:539.

24. **Kahn, M., H. Sugawara, P. McGowan, K. Okuno, S. Nagoya, K. E. Hellström, I. Hellström, and P. Greenberg.** 1991. CD4+ T Cell Clones Specific for the Human p97 Melanoma-Associated Antigen can Eradicate Pulmonary Metastases from a Murine Tumor Expressing the p97 Antigen. *J. Immunol.* *146*:3235.

25. **Brown, J. P., R. M. Hewick, I. Hellström, K. E. Hellström, R. F. Doolittle, and W. J. Dreyer.** 1982. Human melanoma-associated antigen p97 is structurally and functionally related to transferrin. *Nature 296*:171.

26. **Plowman, G. D., J. P. Brown, C. A. Enns, J. Schröder, B. Nikinmaa, H. H. Sussman, K. E. Hellström, and I. Hellström.** 1983. Assignment of the gene for human melanoma-associated antigen p97 to chromosome 3. *Nature 303*:70.

27. **Rose, T. M., G. D. Plowman, D. B. Teplow, W. J. Dreyer, K. E. Hellström, and J. P. Brown.** 1986. Primary structure of the human melanoma-associated antigen p97 (melanotransferrin) deduced from the mRNA sequence. *Proc. Natl. Acad. Sci. USA 83*:1261.

28. **Dippold, W. G., K. O. Lloyd, L. T. C. Li, H. Ikeda, H. F. Oettgen, and L. J. Old.** 1980. Cell surface antigens of human melanoma: Definition of six antigenic systems with monoclonal antibodies. *Proc. Natl. Acad. Sci. USA 77*:6114.

29. **Liao, S. K., P. C. Kwong, and M. J. Khosravi.** 1985. Immunopurification, Characterization, and Nature of Membrane Association of Human

Melanoma-Associated Oncofetal Antigen gp87 Defined by Monoclonal Antibody 140.240. *J. Cell. Biochem.* 27:303.

30. **Real, F. X., K. S. Furukawa, M. J. Mattes, S. A. Gusik, C. Cordon-Cardo, H. F. Oettgen, L. J. Old, and K. O. Lloyd.** 1988. Class 1 (unique) tumor antigens of human melanoma: Identification of unique and common epitopes on a 90-kDa glycoprotein. *Proc. Natl. Acad. Sci. USA 85*:3965.

31. **Furukawa, K. S., K. Furukawa, F. X. Real, L. J. Old, and K. O. Lloyd.** 1989. A Unique Antigenic Epitope of Human Melanoma is Carried on the Common Melanoma Glycoprotein gp95/p97. *J. Exp. Med. 169*:585.

32. **Real, F. X., A. N. Houghton, A. P. Albino, C. Cordon-Cardo, M. R. Melamed, H. F. Oettgen, and L. J. Old.** 1985. Surface Antigens of Melanomas and Melanocytes Defined by Mouse Monoclonal Antibodies: Specificity Analysis and Comparison of Antigen Expression in Cultured Cells and Tissues. *Cancer Res. 45*:4401.

33. **Sciot, R., R. De Vos, P. van Eyken, K. van der Steen, P. Moerman, and V. J. Desmet.** 1989. In situ localization of melanotransferrin (melanoma-associated antigen P97) in human liver. A light- and electronmicroscopic immunohistochemical study. *Liver 9*:110.

34. **Casellas, P., J. P. Brown, O. Gros, P. Gros, I. Hellström, F. K. Jansen, P. Poncelet, R. Roncucci, H. Vidal, and K. E. Hellström.** 1982. Human Melanoma Cells can be Killed *in vitro* by an Immunotoxin Specific for Melanoma-Associated Antigen p97. *Int. J. Cancer 30*:437.

35. Hu, S. L., G. D. Plowman, P. Sridhar, U. S. Stevenson, J. P. Brown, and C. D. Estin. 1988. Characterization of a Recombinant Vaccinia Virus Expressing Human Melanoma-Associated Antigen p97. *J. Virol.* *62*:176.

36. Estin, C. D., U. S. Stevenson, G. D. Plowman, S. L. Hu, P. Sridhar, I. Hellström, J. P. Brown, and K. E. Hellström. 1988. Recombinant vaccinia virus vaccine against the human melanoma antigen p97 for use in immunotherapy. *Proc. Natl. Acad. Sci. USA* *85*:1052.

37. Eisenberg, D., E. Schwarz, M. Komaromy, and R. Wall. 1984. Analysis of Membrane and Surface Protein Sequences with the Hydrophobic Moment Plot. *J. Mol. Biol.* *179*:125.

38. Low, M. G. 1989. The glycosyl-phosphatidylinositol anchor of membrane proteins. *Biochim. Biophys. Acta* *988*:427.

39. Lisanti, M. P., E. Rodriguez-Boulan, and A. R. Saltiel. 1990. Emerging Functional Roles for the Glycosyl-Phosphatidylinositol Membrane Protein Anchor. *J. Membrane Biol.* *117*:1.

40. Ferguson, M. A. J., S. W. Homans, R. A. Dwek, and T. W. Rademacher. 1988. Glycosyl-Phosphatidylinositol Moiety That Anchors *Trypanosoma brucei* Variant Surface Glycoprotein to the Membrane. *Science* *239*:753.

41. Homans, S. W., M. A. J. Ferguson, R. A. Dwek, T. W. Rademacher, R. Anand, and A. F. Williams. 1988. Complete structure of the glycosyl

phosphatidylinositol membrane anchor of rat brain Thy-1 glycoprotein. *Nature 333*:269.

42. **Doering, T. L., W. J. Masterson, G. W. Hart, and P. T. Englund.** 1990. Biosynthesis of Glycosyl Phosphatidylinositol Membrane Anchors. *J. Biol. Chem. 265*:611.

43. **Moran, P. and I. W. Caras.** 1991. A Nonfunctional Sequence Converted to a Signal for Glycophosphatidylinositol Membrane Anchor Attachment. *J. Cell Biol. 115*:329.

44. **Moran, P. and I. W. Caras.** 1991. Fusion of Sequence Elements from Non-anchored Proteins to Generate a Fully Functional Signal for Glycophosphatidylinositol Membrane Anchor Attachment. *J. Cell Biol. 115*:1595.

45. **Keller, G. A., M. W. Siegel, and I. W. Caras.** 1992. Endocytosis of glycophospholipid-anchored and transmembrane forms of CD4 by different endocytic pathways. *EMBO J 11*:863.

46. **Trowbridge, I. S., R. Hyman, and C. Mazauskas.** 1978. The Synthesis and Properties of T25 Glycoprotein in Thy-1-Negative Mutant Lymphoma Cells . *Cell 14*:21.

47. **Ferguson, M. A. J. and A. F. Williams.** 1988. Cell-Surface Anchoring Of Proteins Via Glycosyl-Phosphatidylinositol Structures. *Ann. Rev. Biochem. 57*:285.

48. **Metz, C. N., Y. Zhang, Y. Guo, T. C. Tsang, J. P. Kochan, N. Altszuler, and M. A. Davitz.** 1991. Production of the Glycosylphosphatidylinositol-specific Phospholipase D by the Islets of Langerhans. *J. Biol. Chem. 266*:17733.

49. **Pelham, H. R. B.** 1991. Multiple Targets for Brefeldin A. *Cell 67*:449.

50. **Klausner, R. D., J. G. Donaldson, and J. Lippincott-Schwartz.** 1992. Brefeldin A: Insights into the Control of Membrane Traffic and Organelle Structure. *J. Cell. Biol. 116*:1071.

51. **Lippé, R., E. Luke, Y. T. Kuah, C. Lomas, and W. A. Jefferies.** 1991. Adenovirus Infection Inhibits the Phosphorylation of Major Histocompatibility Complex Class I Proteins. *J. Exp. Med. 174*:1159.

52. **Low, M. G., J. Stiernberg, G. L. Waneck, R. A. Flavell, and P. W. Kincade.** 1988. Cell-specific heterogeneity in sensitivity of phosphatidylinositol-anchored membrane antigens to release by phospholipase C. *J. Immunol. Methods 113*:101.

53. **von Boxberg, Y., R. Wütz, and U. Schwarz.** 1990. Use of the biotin-avidin system for labelling, isolation and characterization of neural cell-surface proteins. *Eur. J. Biochem. 190*:249.

54. **Bordier, C.** 1981. Phase Separation of Integral Membrane Proteins in Triton X-114 Solution. *J. Biol. Chem. 256*:1604.

55. **Estin, C. D., U. Stevenson, M. Kahn, I. Hellström, and K. E. Hellström.** 1989. Transfected Mouse Melanoma Lines That Express Various Levels of Human Melanoma-Associated Antigen p97. *J. Natl. Cancer Inst. 81*:445.

56. **Low, M. G. and P. W. Kincade.** 1985. Phosphatidylinositol is the membrane-anchoring domain of the Thy-1 glycoprotein. *Nature 318*:62.

57. **Takami, N., K. Oda, T. Fujiwara, and Y. Ikehara.** 1990. Intracellular accumulation and oligosaccharide processing of alkaline phosphatase under disassembly of the Golgi complex caused by brefeldin A. *Eur. J. Biochem. 194*:805.

58. **Urbani, L. and R. D. Simoni.** 1990. Cholesterol and Vesicular Stomatitis Virus G Protein Take Separate Routes from the Endoplasmic Reticulum to the Plasma Membrane. *J. Biol. Chem. 265*:1919.

59. **Vance, J. E., E. J. Aasman, and R. Szarka.** 1991. Brefeldin A Does Not Inhibit the Movement of Phosphatidylethanolamine from Its Sites of Synthesis to the Cell Surface. *J. Biol. Chem. 266*:8241.

60. **Rothberg, K. G., Y. Ying, J. F. Kolhouse, B. A. Kamen, and R. G. W. Anderson.** 1990. The Glycophospholipid-linked Folate Receptor Internalizes Folate Without Entering the Clathrin-coated Pit Endocytic Pathway. *J. Cell Biol. 110*:637.

61. **Anderson, R. G. W., B. A. Kamen, K. G. Rothberg, and S. W. Lacey.** 1992. Potocytosis: Sequestration and Transport of Small Molecules by Caveolae. *Science 255*:410.

62. **Rothberg, K. G., J. E. Heuser, W. C. Donzell, Y. S. Ying, J. R. Glenney, and R. G. W. Anderson.** 1992. Caveolin, a Protein Component of Caveolae Membrane Coats. *Cell 68*:673.

63. **Baker, E. N., H. M. Baker, C. A. Smith, M. R. Stebbins, M. Kahn, K. E. Hellström, and I. Hellström.** 1992. Human melanotransferrin (p97) has only one functional iron-binding site. *FEBS LETTERS 298*:215.

64. **Anderson, B. F., H. M. Baker, G. E. Norris, S. V. Rumball, and E. N. Baker.** 1990. Apolactoferrin structure demonstrates ligand-induced conformational change in transferrins. *Nature 344*:784.

65. **Woodworth, R. C., A. B. Mason, W. D. Funk, and R. T. A. MacGillivray.** 1991. Expression and Initial Characterization of Five Site-Directed Mutants of the N-Terminal Half-Molecule of Human Transferrin. *Biochemistry 30*:10824.

66. **McGraw, T. E., L. Greenfield, and F. R. Maxfield.** 1987. Functional Expression of the Human Transferrin Receptor cDNA in Chinese Hamster Ovary Cells Deficient in Endogenous Transferrin Receptor. *J. Cell Biol. 105*:207.

67. **Lisanti, M. P., A. Le Bivic, A. R. Saltiel, and E. Rodriguez-Boulan.** 1990. Preferred Apical Distribution of Glycosyl-Phosphatidylinositol (GPI)

Anchored Proteins: A Highly Conserved Feature of the Polarized Epithelial Cell Phenotype. *J. Membrane Biol. 113*:155.

68. **Lisanti, M. P., I. W. Caras, M. A. Davitz, and E. Rodriguez-Boulan.** 1989. A Glycophospholipid Membrane Anchor Acts as an Apical Targetting Signal in Polarized Epithelial Cells. *J. Cell Biol. 109*:2145.

69. **Alvarez-Hernandez, X., G. M. Nichols, and J. Glass.** 1991. Caco-2 cell line: a system for studying intestinal iron transport across epithelial cell monolayers. *Biochim. Biophys. Acta 1070*:205.

70. **Štefanová, I., V. Hořejší, I. J. Ansotegui, W. Knapp, and H. Stockinger.** 1991. GPI-Anchored Cell-Surface Molecules Complexed to Protein Tyrosine Kinases. *Science 254*:1016.

71. **Majerus, P. W., T. S. Ross, T. W. Cunningham, K. K. Caldwell, A. B. Jefferson, and V. S. Bansal.** 1990. Recent Insights in Phosphatidylinositol Signaling. *Cell 63*:459.